

1949

# Plastic behavior of continuous beams, Lehigh University, (1949) M.S.

C. H. Yang

Follow this and additional works at: <http://preserve.lehigh.edu/engr-civil-environmental-fritz-lab-reports>

---

## Recommended Citation

Yang, C. H., "Plastic behavior of continuous beams, Lehigh University, (1949) M.S." (1949). *Fritz Laboratory Reports*. Paper 1313.  
<http://preserve.lehigh.edu/engr-civil-environmental-fritz-lab-reports/1313>

This Technical Report is brought to you for free and open access by the Civil and Environmental Engineering at Lehigh Preserve. It has been accepted for inclusion in Fritz Laboratory Reports by an authorized administrator of Lehigh Preserve. For more information, please contact [preserve@lehigh.edu](mailto:preserve@lehigh.edu).

T A B L E S

- I. Test coupon result
- II. Coupon results

FIGURES

- 1. Set-up of simple beam control test.
- 2. Set-up of continuous beam test.
- 3. The dynamometers and Hydraulic jack assembly for loading the continuous beam.
- 4. Lateral support frame for continuous beam tests.
- 5. Detail of vertical support in continuous beam test.
- 6. Continuous Beam test set-up.
- 7. Deflection and strain gage locations. Test B-1.
- 8. Deflection strain and level gage locations. Test B-2.
- 9. Deflection strain and level gage locations. Test B-3.
- 10. Moment -  $\phi$  curve. Test B-1. (Plotted from deflection gage data.)
- 11. Moment -  $\phi$  curve. Test B-1. (Plotted from strain gage data.)
- 12. Load deflection curve. Test No. B-1.
- 13. Load strain curves. Test No. B-3.
- 14. Load strain curves. Test No. B-3.
- 15. Load deflection curve. Test No. B-2.
- 16. Load deflection curve. Test No. B-3.
- 17. Moment angle curve. Test No. B-3.
- 18. Moment deflection curve. Test No. B-3.
- 18A. Deflection contour curve. Test No. B-3.
- 19. Load moment curve. Test No. B-2.
- 20. Moment -  $\phi$  curve. Test No. B-2.
- 21. Moment -  $\phi$  curve. Test No. B-3.
- 22. Moment -  $\phi$  curve. Test No. B-3.

23. End moment - moment at central section. Test No. B-3.
24. Lueder lines developed around the support of continuous beam B-2 at a load  $W = 44$  kips.
25. Flow lines commencing on the top flange of the central span at a load  $W = 46$  kips in continuous beam B-2.
26. The progression of Lueder lines on the top flanges of the central span at a load  $W = 47$  kips in continuous beam test B-2.
27. Lueder lines appearing on the lower flange of the central span at a load  $W = 50.5$  kips. Test B-2.
28. The progression of Lueder lines in the lower flange of the central span at a load  $W = 54$  kips in continuous beam test B-2.
29. Side view of central span, continuous beam B-2 after test.
30. Moment  $\phi$  curve. Test No. B-3.
31. Local buckling of lower flange near support in continuous beam B-2.
32. Lueder line patterns in the cantilever portion of continuous beam B-3 showing the penetration of plastic zone into the web at a load  $W = 51$  kips.
33. Load-lateral rotation curve. Test No. B-3.
34. Continuous beam B-3 twisted after test due to lateral buckling.
35. Lines developed by local shear failure in web near the support at a load  $W = 39$  kips. Continuous beam test B-3.
36. Progression of shear yielding in the web.  $W = 47.5$  kips, test B-3.
37. Progression of Lueder lines developed in the web by shear failure at a load  $W = 48$  kips. Test B-3.
38. Shear pattern of continuous beam B-3.  $W = 51$  kips.
39. Lueder line pattern of continuous beam B-3 after test.
40. Load - strain curves for shear gages. Test No. B-3.
41. Strain distribution at section B'. Test No. B-2.
42. Strain distribution at section B2. Test No. B-2.
43. Strain distribution at section B. Test No. B-2.
44. Strain distribution at section B1. Test No. B-2.

45. Moment -  $\phi$  curves. Test No. B-2.
46. Moment -  $\phi$  curves. Test No. B-3.
47. The increment of deflection from  $W = 5$  kips to  $W = 25$  kips under repeated load. Test No. B-5.
48. Increment of initial deflection under repeated load. Test No. B-5.
49. Tension and compression stress-strain curves for an 8WF40 beam.
50. Tension stress-strain curves for an 8WF40 beam. (Including strain-hardening range.)



Had occasion to  
read this report ~  
not too carefully ~  
but noted <sup>a few</sup> ~~some~~ errors  
- also some questionable  
points.

Some of the errors  
perhaps should be  
corrected before report  
goes to Baker + Moon,  
particularly, the  
incorrect use of the  
word "effected" - P.C.

Ultimate Strength of Welded Continuous Frames  
and their Components

Progress Report B

PLASTIC BEHAVIOR OF CONTINUOUS BEAMS

By

C. H. Yang

This report to the Lehigh  
Project Subcommittee presents  
results of the tests. It is  
for information only.

NOT FOR PUBLICATION

Fritz Engineering Laboratory  
Civil Engineering Department  
Lehigh University

May 26, 1949

## INTRODUCTION

The present investigation was undertaken in order to obtain information on steel WF continuous beams tested from the elastic range through the plastic range until ultimate strength was developed. Special interest has been given to the study of:

- a. Redistribution of stress in the beam after a portion of it went to the plastic range.
- b. The combined effect of stress concentration, residual stresses, and the change of mechanical properties in the heat effected zone in the beam due to welding on the general behavior of continuous beams in both elastic and plastic range.

Brief discussions are also included in this report which consider the effects of lateral buckling, strain hardening and local buckling on the ultimate strength of continuous beams.

Since the program is only partially completed, this report will emphasize the information observed on the tests completed thus far. Three tests were made as shown in the following table. One was tested as a simple beam to provide the basic information for the analysis of the results of the continuous beams.

Test No.	Type of Test	Size of Member	Distance between Supports	Load
B <sub>1</sub>	Simple beam control	8WF40	14'	1/3 point
B <sub>2</sub>	Continuous beam with central span fully restrained <sup>(1)</sup>	8WF40	14'	1/3 point
B <sub>3</sub>	Continuous beam simulating rigid frame. <sup>(2)</sup>	8WF40	14'	1/3 point

(1) Force at end of cantilever sections regulated to keep beam level over support point.

(2) Cantilever load regulated to keep end in same horizontal plane as support points.

Test Specimens B<sub>2</sub> and B<sub>3</sub> were made from a single member 8WF40 section and were tested in the as-rolled condition. One-half inch thick stiffener plates were fillet-welded to the web at the supports and loading brackets were welded at the loading points as was done in previous simple beam tests.

Deflection, angle rotation and strain were measured by Ames dials, level bars and SR-4 strain gages located as shown in Figs. 6, 7, 8, & 9.

#### TEST SET UP AND TESTING PROCEEDURE

The same apparatus was adopted in the control test as described in the previous progress report "Plastic Behavior of Wide Flange Beams". Fig. 1 shows the general view of the test set up.

A new set up was designed for testing continuous beams. The general arrangement of test is shown in Figs. 2 & 6. The specimen was supported on two rollers as shown

in Fig. 5. A deflection gage rig was attached to plates for mounting of Ames dial gages.

Four hydraulic jacks were used for loading. Aluminum tube dynamometers were designed and calibrated for measuring the load. Forces were applied by jacks and dynamometers connected between the loading bracket of the specimens and the base beam as shown in Fig. 3.

A lateral bracing frame was used for the prevention of lateral deflection as shown in Figs. 4 & 6.

Load was applied by hand pumps.

Load was kept constant during the time that readings were taken. Curves of some deflection gage and strain gage data were plotted during the test for general information.

In the plastic range, yielding proceeds very slowly. Unless the test procedure were modified, considerable time would elapse before absolute static equilibrium conditions were obtained. A criterion was adopted for taking readings under such circumstances as follows: When the increase of deflection in the central dial gage of the beam was less than .002" within 15 minutes, a whole set of readings could be taken. The test then proceeds with another increment of load.

## RESULTS AND DISCUSSIONS

### A. Initial Yield Strength and Ultimate Strength of the Control Test (E1)\*

M -  $\phi$  curves of the central section of the beam are plotted in Figs. 10 and 11. The load deflection curve is shown in Fig. 12.

The observed and calculated initial yielding strengths are tabulated as follows:

	<u>Initial Yield Strength</u>		<u>Ultimate Strength</u>	
	<u>Load</u>	<u>Moment</u>	<u>Load</u>	<u>Moment</u>
Observed from load deflection curves	27.5 kips	770 in.kips	50.3 kips	1406 in. kips
Observed from M - $\phi$ curves	42.8 kips	1200 in.kips	50.3 kips	1406 in. kips
Calculated	46.2 kips	1294 in.kips	55.4 kips	1550 in. kips

The initial yield strength of the beam as observed from Fig. 12 is about 27.5 kips corresponding to a moment of 770 inch-kips. This load value observed from the load deflection curve is apparently due to local yielding around the loading brackets and is probably induced from welding residual stress and stress concentration. The remaining parts of the beam are still in the elastic range at this load as shown by M -  $\phi$  curves in Figs. 10 and 11.

At a load of 38.5 kips, yield lines were observed on the upper flange of the beam between the two load points. The whole central span probably started to yield at this load. The M -  $\phi$  curves (Figs. 10, 11) show an initial yield load of 42.8 kips which is very close to this load. The lowering of the

\* The term "load" in this section only, refers to total load on the simple beam.

BT suggest "cooling".

- 5 -

initial yield strength of the whole section from that predicted might be due to rolling residual stresses.

The ultimate strength of the beam section is about 9% lower than calculated. Similar results were reported in Progress Report No. 1, "Plastic Behavior of WF Beams".

#### B. Initial Yield Strength of Continuous\*Beams

The exact load at initial yield in actual structures is difficult to determine. Due to such factors as stress concentration and residual stresses structures do not behave in perfect elastic fashion even at low loads.

The initial yield strengths of the continuous beams in this report are estimated from the change of slope in the load displacement curves.

In both test No. B2 and B3, the whitewash near the supports started to show Lueder lines at a load 50% below the data from the calculated yield load. The strain gages on the top flange of continuous beam B3 at the load and support points are plotted in Figs. 13 and 14. Local yield is observed at a load  $W = 21$  kips.

The general behavior of the beam is not significantly affected by such local yielding as can be seen from the load-displacement curves shown in Figs. 15 to 18.

The calculated and observed initial yield strengths are tabulated as follows:

-----

\* The term "load" in this section refers to load in one dynamometer.

<u>Initial Yielding Strength</u>		
	<u>Calculated</u>	<u>Observed</u>
B2	W = 34.7 kips	W = 27 kips
B3	W = 46.2 kips	W = 39 kips

Different bending strengths were observed at the two support points of beam B2. End moments are plotted against load in Fig. 19. The east end started to yield at lower load than the west end.

$M = \phi$  curves are plotted from strain and deflection gages for tests B2 and B3, Figs. 20 - 22. It is clear that  $M - \phi$  curves would be affected by residual stresses due to rolling through the whole length of the beam but generally will not be affected by the local failures.

These curves show an apparent higher initial yield strength than the values observed from load displacement curves (Figs. 15 - 18).

In Fig. 22, data from gages 43 and 44 shows increased  $\phi$  for a lower resisting moment. Eventually it developed the same strength as at other sections as plastic yielding progressed. This is evidence that residual stress does not decrease  $M_p$ .

After the initial yield strength of a beam is reached, redistribution of moment occurs. For example, in a restrained beam, yielding at the supports is accompanied by a distribution of increased moment to the central span upon subsequent loading. The end moments are relaxed as a result of plastic flow caused by residual stresses and stress concentration near the support.

? (BJ)



① BJ

'This was true in one test.  
No general conclusion  
can be made. Depends  
on location on cooling bed

For test B2 the end moments and moment at the central section are plotted in Fig. 19. The tangent straight lines are values calculated in the elastic range.

The central span in both tests are continuous with overhanging ends. Only 1/4" fillet welds were applied to the stiffener plates at the supports. In the future program butt welds at the supports will be studied.

In test B3 and moments are plotted against the moment of the central section in Fig. 23. The curve closely follows a straight line up to the plastic range.

In both cases it seems that the relaxation of end moments due to plastic flow resulting from welding residual stress and stress concentration at the end supports ~~are~~ small.

Lueder lines were first observed in the upper flange in the central span in continuous beam B2 at a load  $W = 46$  kips. The lines appeared in lower flanges at a higher load,  $W = 50.5$

kips. This may be due to the combined effects of a slightly higher tensile strength observed in coupon tests (see appendix) and the rolling residual stress distribution. The compressive residual strains observed along flange edges are higher than tensile strains. This was described in Progress Report No. 1. A set of pictures are shown in Figs. 25 to 29 to show the development of Lueder lines on both flanges in test B2.

### C. Ultimate Strength of Continuous Beams

The ultimate strength of a structure as defined by the general plastic ~~design~~ theory is a limiting load that the structure can withstand.

In estimating this limiting value no consideration is given to the deflections of the structure. Also, it would be impossible in some structures to approach this limiting value.

Furthermore, some yielded portions of the structure might become strain hardened which is also not considered in the usual theory. This changes the behavior of the structure.

In both tests B2 and B3, the limiting ultimate load was estimated as the load which would develop plastic hinges in the two supports and in the central span as follows:

$$W = \frac{2M_p}{L/3} = 50 \text{ kips}$$

Where  $L$  = length central span

$M_p$  = Limiting resisting moment for the  
section = 1400 in-kips (From the  
control test).

$M - \phi$  curves are plotted from strain and deflection gages for both tests in Fig. 20 - 22.  $M - \phi$  curves are also plotted from strain gages in cantilever beams in Figs. 30 and 45. They all show good agreement with the result obtained in <sup>the</sup> control test. Different depth of plastic zone penetration in the web of <sup>the</sup> cantilever beam under different resisting moment in test B3 is shown in Fig. 32.

In Fig. 19 end moments were plotted against load for test B2. Plastic hinges were formed at the supports after the

Not a design theory. Either  
① design Method  
② Plastic Theory.

Hauskoff takes strain-hardening into account.

How do these curves show this?

end moment reached the limiting resisting moment. At a load  $W = 46$  kips the central constant moment section started to yield which reduced the rigidity of the beam and this rapidly brought the beams at the supports into the strain hardening range. The end moments increased above  $M_p$  before a plastic hinge was fully developed at the central section. The maximum observed load  $W = 56$  kips on the structure is, thus, higher than predicted (50.0 kips) because of strain hardening at the two supports of the beam.

The load-deflection curve plotted in Fig. 15 shows, approximately, two straight lines in the first part of the curves. The first straight line represents the load deflection relation of the restrained beam before the initial yield strength has been reached. The second straight line indicates the behavior after the ends became plastic hinges and prior to yielding at the center.

End moments are plotted against the moment at the central section for test No. B3 in Fig. 23 showing that the two end moments were only slightly raised by strain hardening. The observed maximum load applied to the beam was 49 kips which is very close to the predicted value. Whereas in B2 there were two straight lines in the load deflection curve, in B3 there was only one (Fig. 16). This is because in the latter case the supports and the central section (under constant moment) reached the initial yield strength at the same time.

curve (B5)?

The deflection contour for test B3 is shown in Fig. 18A.

Inelastic local buckling and lateral buckling may affect the ultimate strength and is discussed briefly as follows:

(1) Inelastic local buckling

When stresses exceed the yield point, some portions of beam flanges under compression may buckle inelastically. The results of an analytical study\* of this problem show that local inelastic buckling may in some cases prevent the section from approaching the limiting resisting moment.

The lower flange at the support of beam B2 failed in this fashion as shown in Fig. 31.

(2) Lateral Buckling

Lateral buckling strength is severely reduced in the plastic range which is also reported in some investigations in England.

The two continuous beams tested buckled laterally in the plastic range in spite of the lateral support provided (Fig. 4). Two level bars were mounted on continuous beam B3 to measure the lateral rotation of the beam. The load-lateral rotation curve is plotted in Fig. 33. The beam buckled in two half-waves between the three lateral support points in the central span at a load  $W = 47$  kips. The beam was twisted after test due to lateral buckling. A picture of the twisted beam is shown in Fig. 34.

---

\* To be included in a later report.

The lateral support frame had, however, prevented the beam from collapsing due to this deformation. Thus, the limiting bending resisting moment was approached in the beam sections as can be seen from the  $M - \theta$  curves plotted in Figs. 20 - 22.

The torsional stresses developed by lateral buckling are revealed by yield lines as shown in Fig. 34A.

#### D. Shear Failure in Beams

By the maximum shear failure hypothesis of the web beam will start to yield by shear as soon as the shear stress in the neutral axis reaches the value

$$\tau = 1/2 \sigma_{yp}$$

where  $\sigma_{yp}$  = yield point stress of web material in a simple tension test = 38.72 kips per sq. in.

The corresponding load in the continuous beam will then be

$$W = \frac{bI}{Q} \sigma_{yp} = 51.3 \text{ kips}$$

where  $W$  = load at each of the loading points in the central span.

$b$  = Web thickness = 0.383 in.

$I$  = Moment of inertia of the beam section about its neutral axis = 142.3 in.

$Q$  = Static moment of beam section about the neutral axis = 41.05 in<sup>3</sup>.

The local shear yielding lines were observed in Test No. B3 at a load  $W = 39$  kips, which is shown in strain gage data Fig. 35. The Lueder lines began to extend in the web at a load

of  $W = 45$  kips. A series of pictures were taken to show the development of shear yielding in the web (Figs. 35 to 39). From shear strain gage data plotted in Fig. 40 it is seen that the web started to yield at a load  $W = 45$  kips. However, at this load the magnitude of shear strains measured had not yet reached the yield point value. Thus, it appears that yielding occurred elsewhere at 45 kips, the area under the gages not yielding until a load  $W = 51$  kips had been reached.

Strain distributions at various loads and at several cross sections of the beam are plotted in Figs. 41 to 44 for beam B2. In the central section under constant moment without shear (Fig. 41) it is seen that the strain distribution remained plane even after the beam flanges went far into plastic range. But in sections under high shear, strain distributions became irregular after shear failure occurs. This is shown in Figs. 42 and 43. Fig. 44 shows the strain distribution of a section on the cantilever beam which was under small shearing force and in which the web was not yielded by shearing stress.

Some analytical study has been made on the problem of shear failure in beams. It has been shown that shear failure in the web would cause a redistribution of normal bending stress along the section and the yielding and ultimate strength of the section under bending is reduced.  $M - \phi$  curves were plotted from strain gage data in both test No. B2 and B3, Figs. 45 & 46. These show the reduction of bending strength after shear failure occurred in the webs. For the symmetric reaction on the cantilever beam, which is under small shear load with the web still in elastic range, curve were also plotted for comparison.

E. Repeated Loading After the Beam Has Been Loaded into the Plastic Range

The continuous beam B3 was repeatedly loaded between a load of  $W = 3$  kips and  $W = 23$  kips as shown below. The upper limit of load was chosen to make the maximum moment in the central span a little higher than initial yielding moment but lower than the maximum moment reached during the continuous beam test.

The test was made to see if the beam behaved elastically and if the deflection of the beam would remain constant. Decreasing deflection between the loads  $W = 3$  kips and  $W = 23$  kips was observed in the first few loading cycles as is plotted in Fig. 47.

The permanent set at initial load was increasing during the same cycles of loading as shown in Fig. 48. It is evident that not enough repetitions of load were applied to definitely establish that the curves in Figs. 47 and 48 were approaching a limit. Repeated load tests will be made in succeeding continuous beam tests to further explore this important subject.



## APPENDIX

### Coupon Test Results

Thirty-seven tension and compression coupon tests were made for determining the mechanical properties of the material. Specimens were cut in different locations in the cross section of the beams.

Some of the tests were carried far into the plastic range to observe the strain hardening effect. Very slow testing speeds were adopted (strain rate = 1 micro-inch per inch strain per second.  $1 \times 10^{-6}$  .000001)

Typical results are presented in Figs. 49 and 50.

Results are tabulated as follows:

### TEST COUPON RESULTS

Table I

Tension Tests			Compression Tests		
Coupon No.	Upper Yield Point	Lower Yield Point	Coupon No.	Upper Yield Point	Lower Yield Point
FL-1	37.1	37.1	FL-1	38.4	38.2
FL-2	36.7	36.5	FL-2	37.7	37.4
FL-3	35.0	35.0	FL-3	39.6	39.4
FL-4	35.2	34.7	FU-1	35.9	35.9
FL-5	40.8	40.6	FU-2	37.2	37.2
FU-1	38.3	38.1	FU-3	37.0	36.8
FU-2	37.5	37.5	Average	37.63	37.35
FU-3	37.9	37.7			
FU-4	38.3	38.1	W-1	34.4	34.2
FU-5	40.7	40.2	W-2	39.2	39.1
Average	37.75	37.55	W-3	38.9	38.9
			W-4	38.2	38.1
W <sub>1</sub>	38.6	38.4	W-5	39.7	39.3
W <sub>2</sub>	39.7	39.3	Average	38.08	37.92
W <sub>3</sub>	42.2	41.7			
W <sub>4</sub>	40.0	39.9			
W <sub>5</sub>	38.3	38.3			
Average	39.76	39.52			

# COUPON RESULTS

Table II\*

T e n s i o n    T e s t s		
Coupon No.	Upper Yield Point	Lower Yield Point
FL-1	38.5	38.3
FL-2	37.7	37.5
FL-3	37.0	36.9
FL-4	37.1	36.9
FU-1	39.4	39.0
FU-2	37.5	37.5
FU-3	37.0	37.0
FU-4	37.5	37.4
Average	37.71	37.56
W-1	38.4	38.4
W-2	39.6	39.6
W-3	37.4	37.4
Average	38.47	38.47

\* Test carried into the strain hardening range.

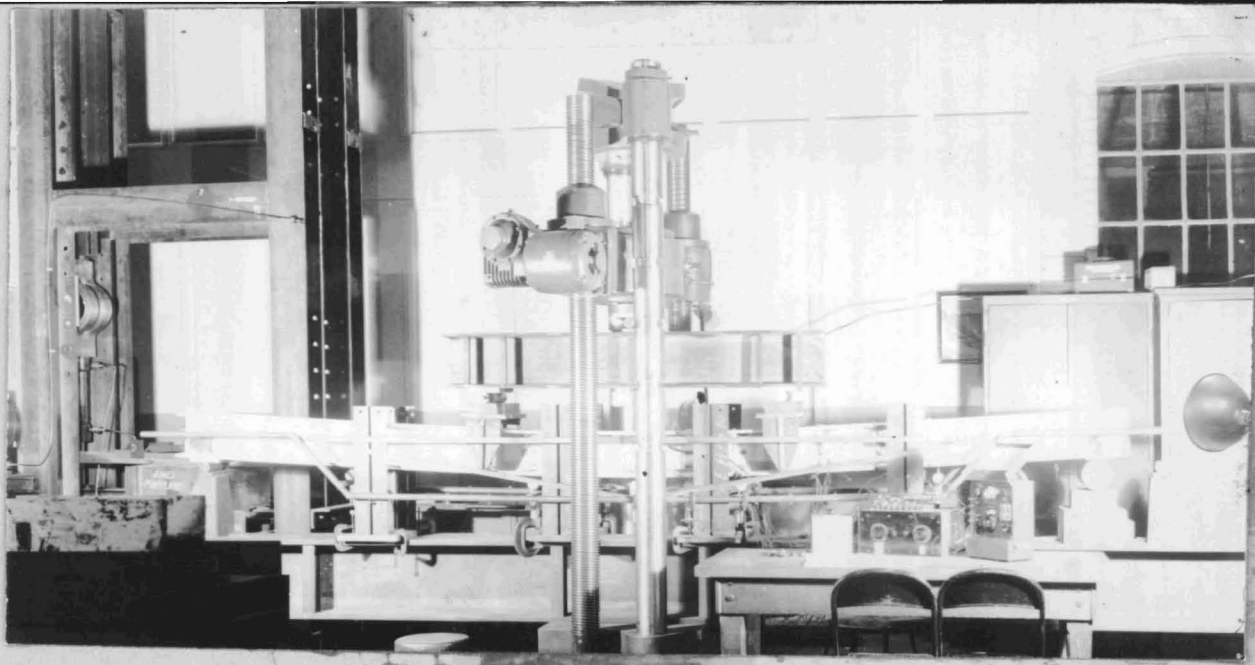


Fig. 1. Set up of simple beam control test.

Fig. 2. Set up of continuous beam test.



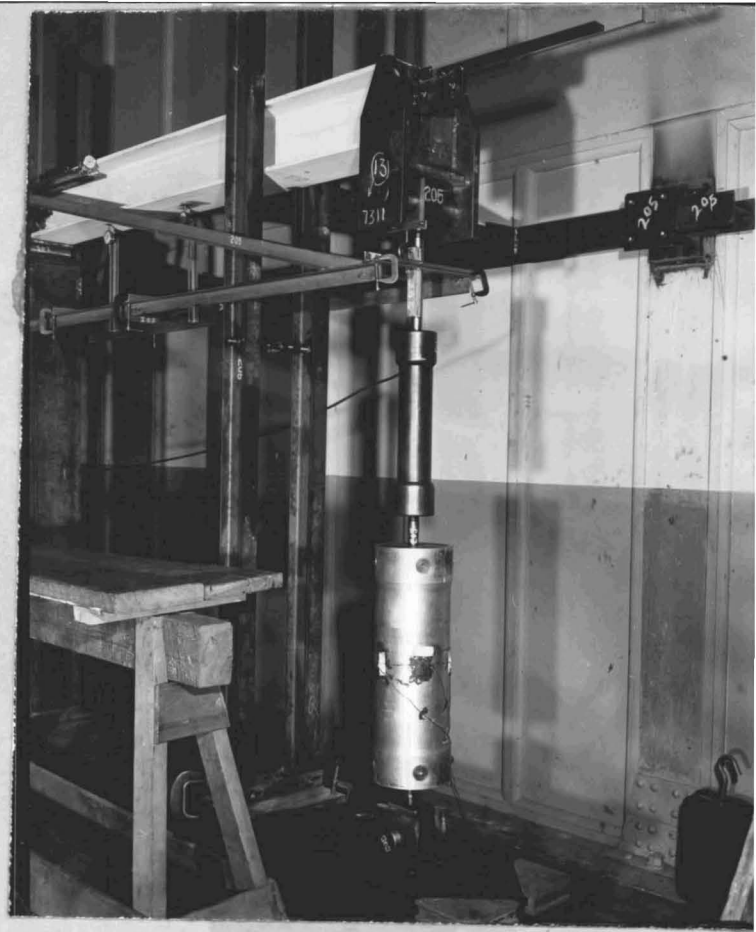


Fig. 3, The dynamometer and hydraulic jack assembly for loading the continuous beam.

Fig. 4. Lateral support frame for continuous beam tests.



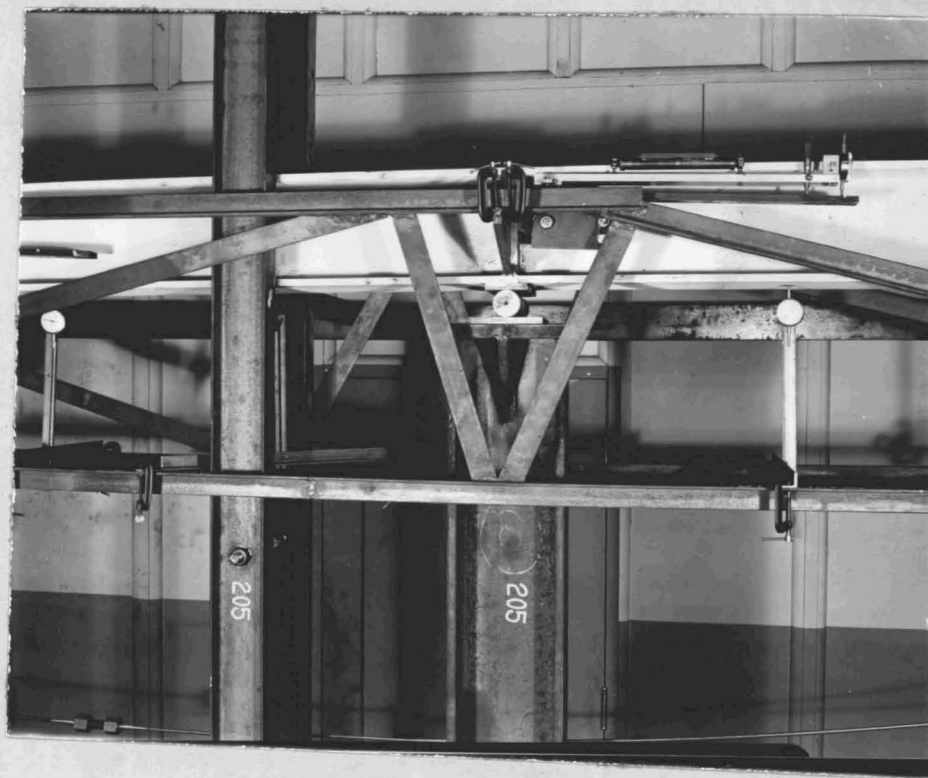
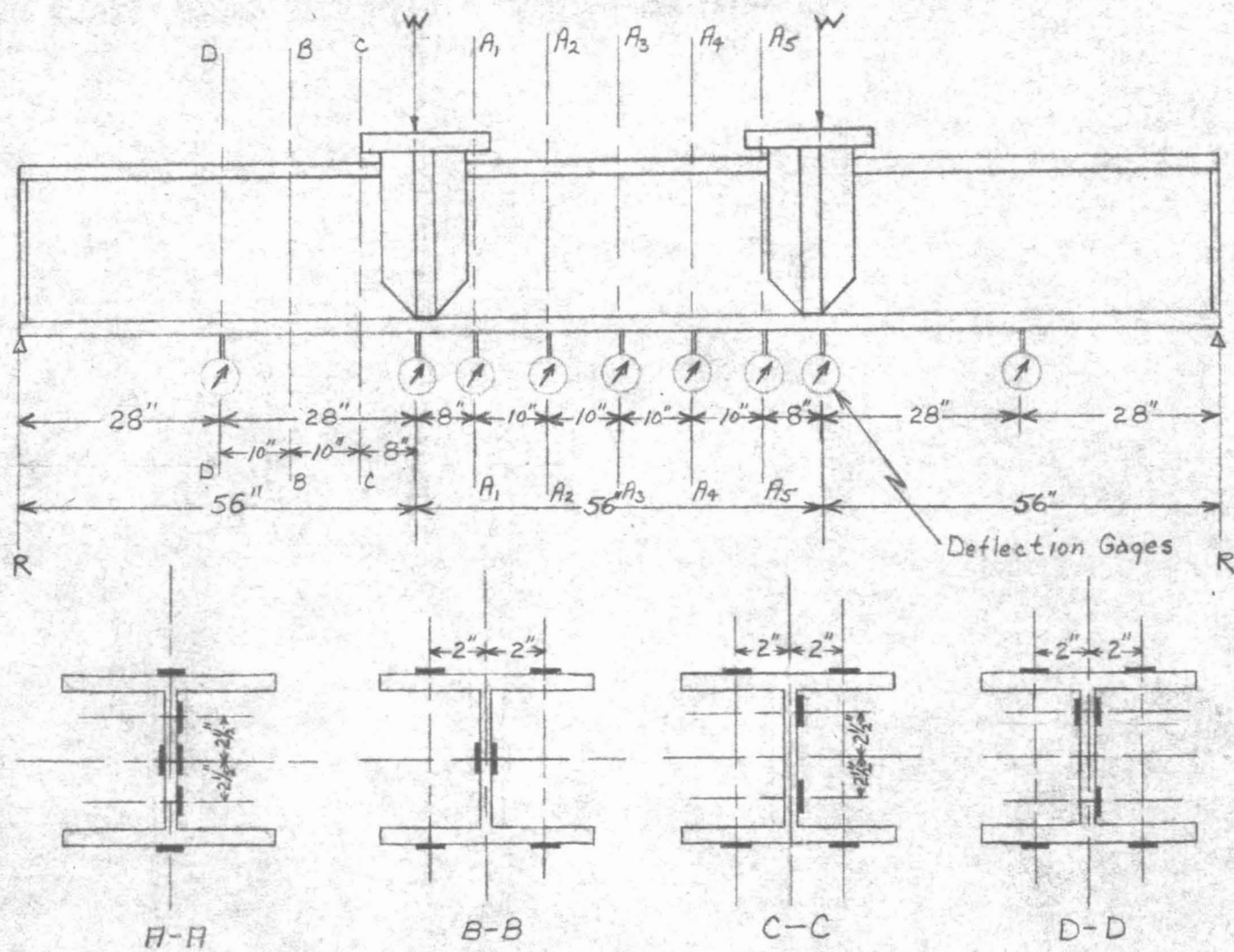


Fig. 5. Detail of vertical support in continuous beam test.

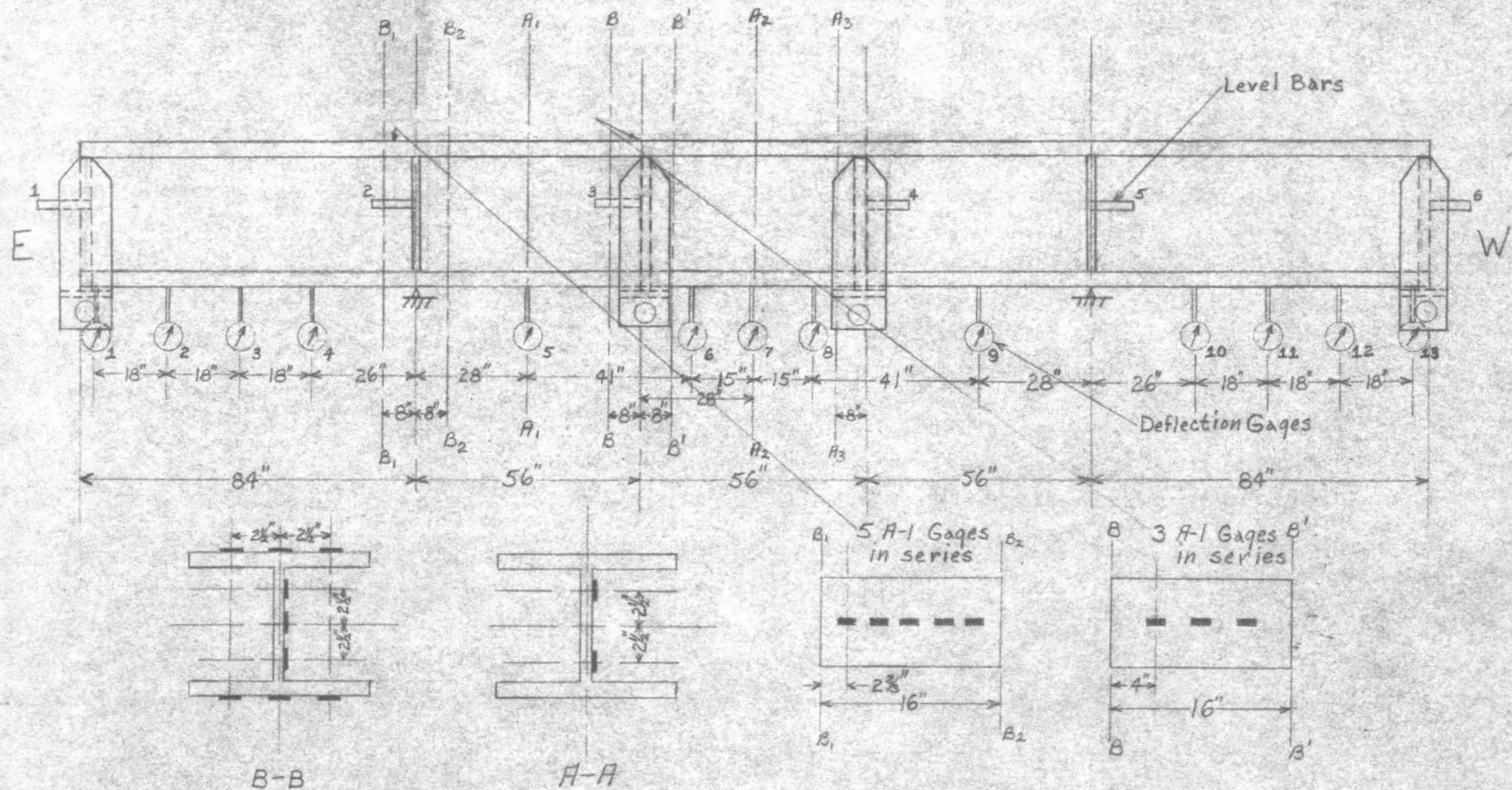






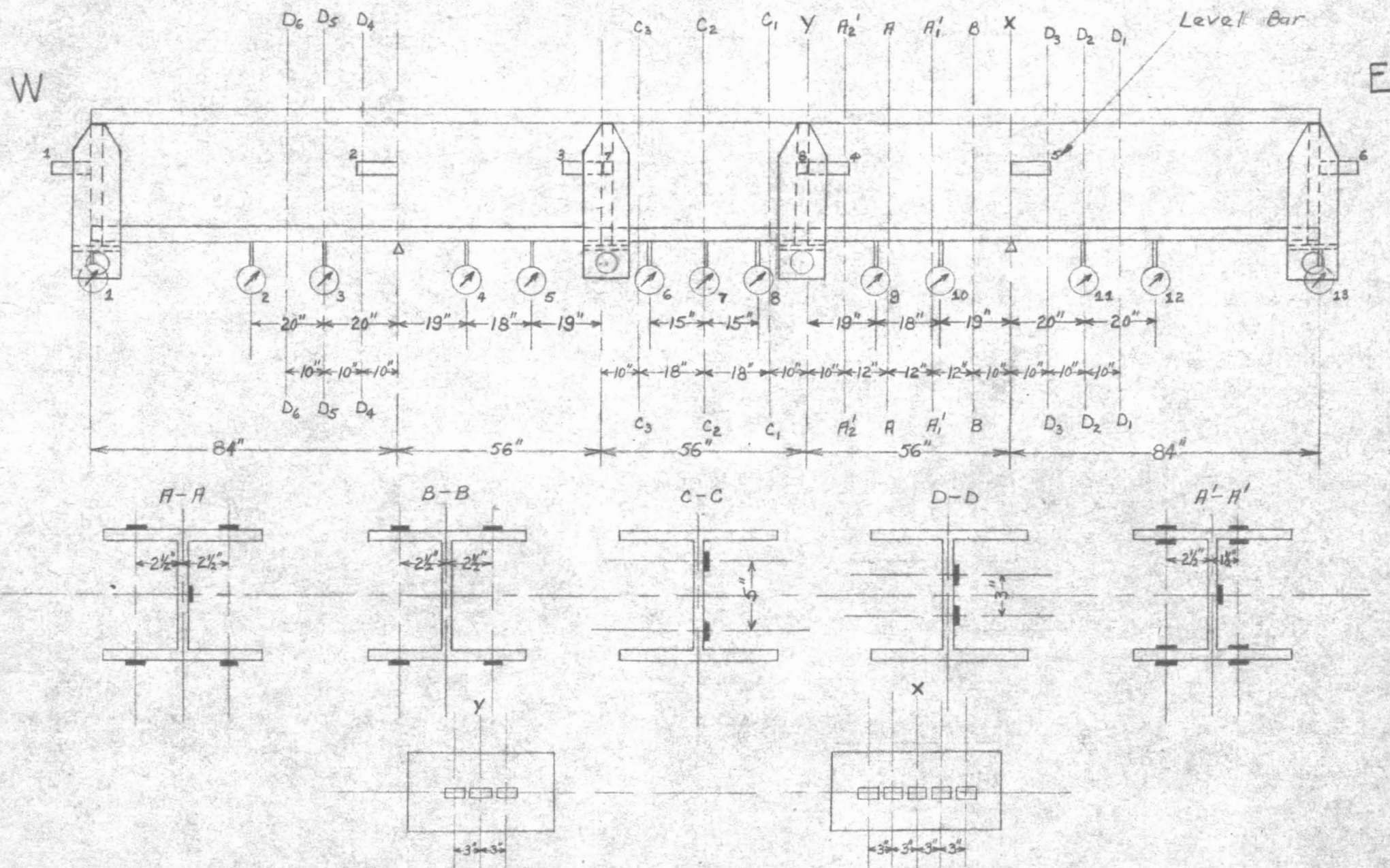
Test No. B-1  
 Fig. 7  
 Deflection and Strain  
 Gage Locations



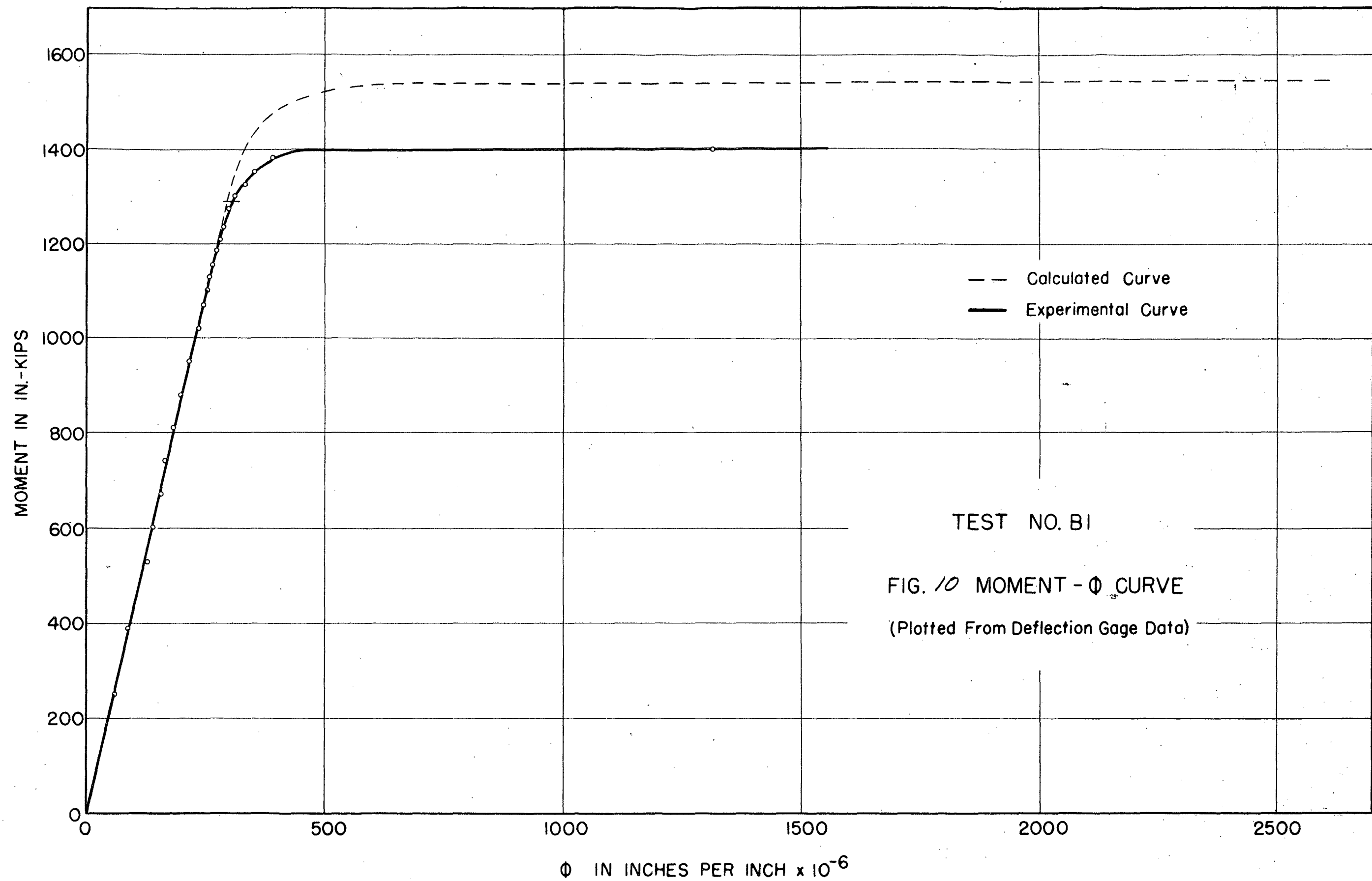


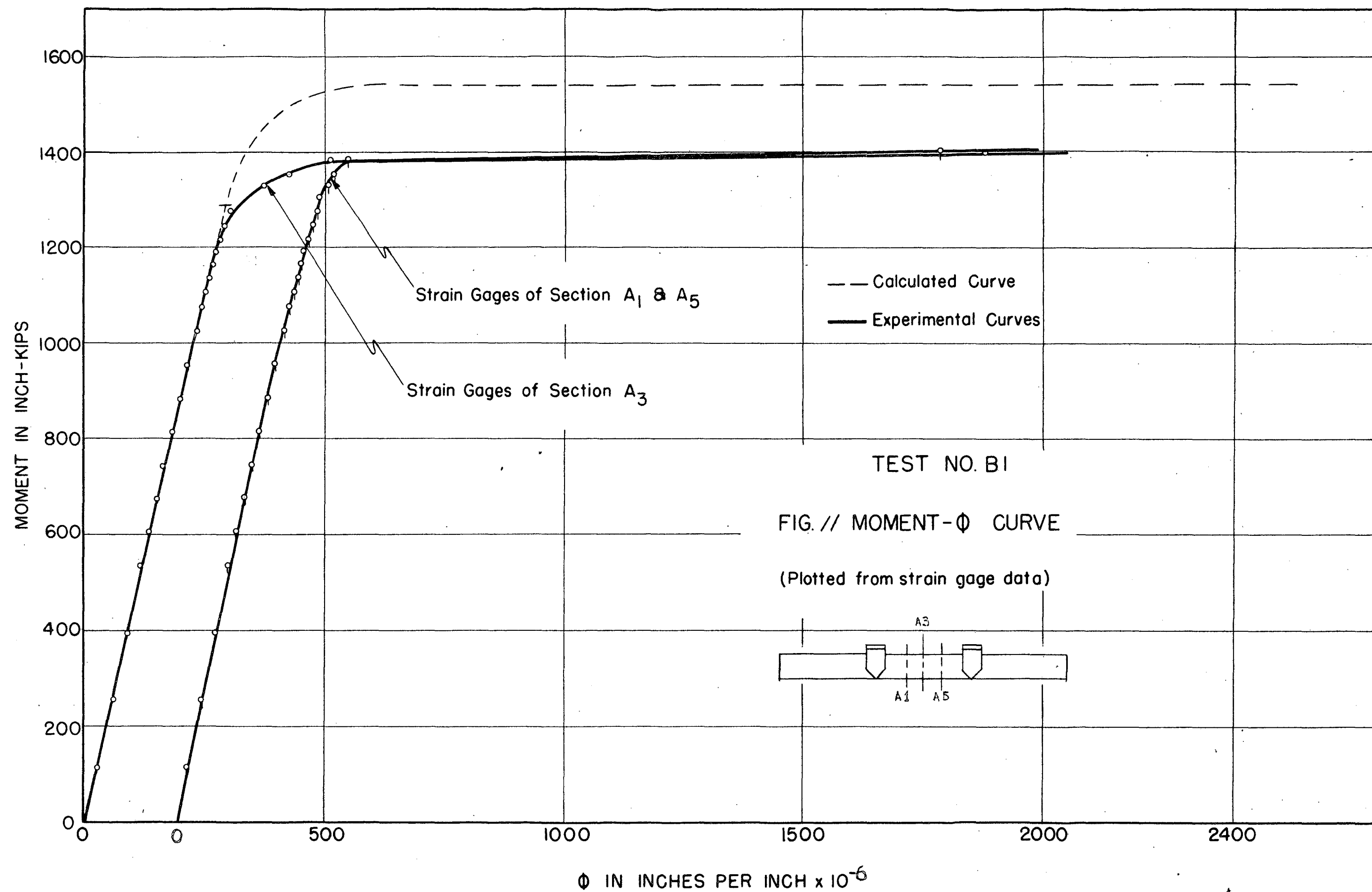
Test B2  
Fig. 8  
Deflection Strain and Level  
Gage Locations

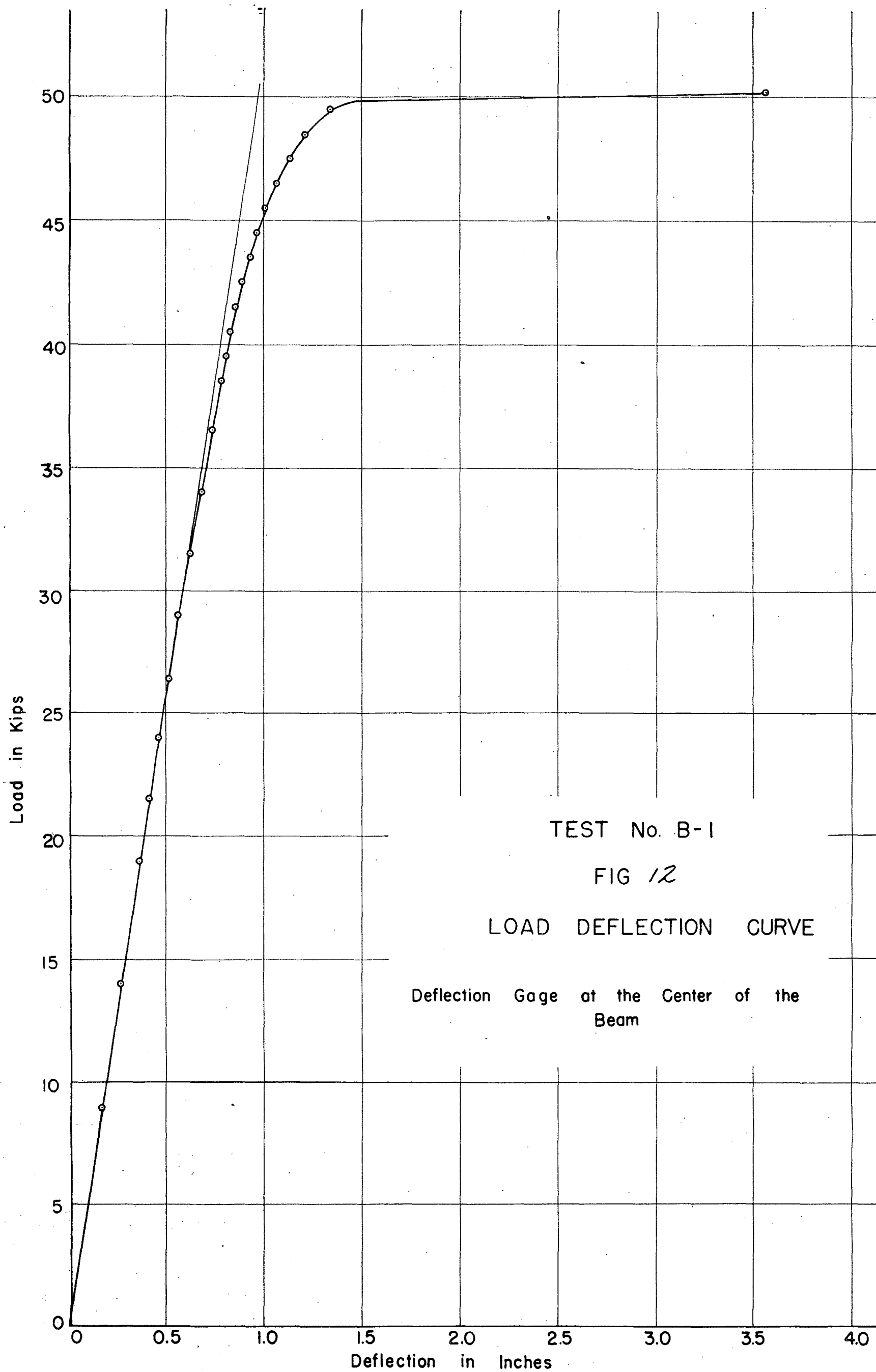


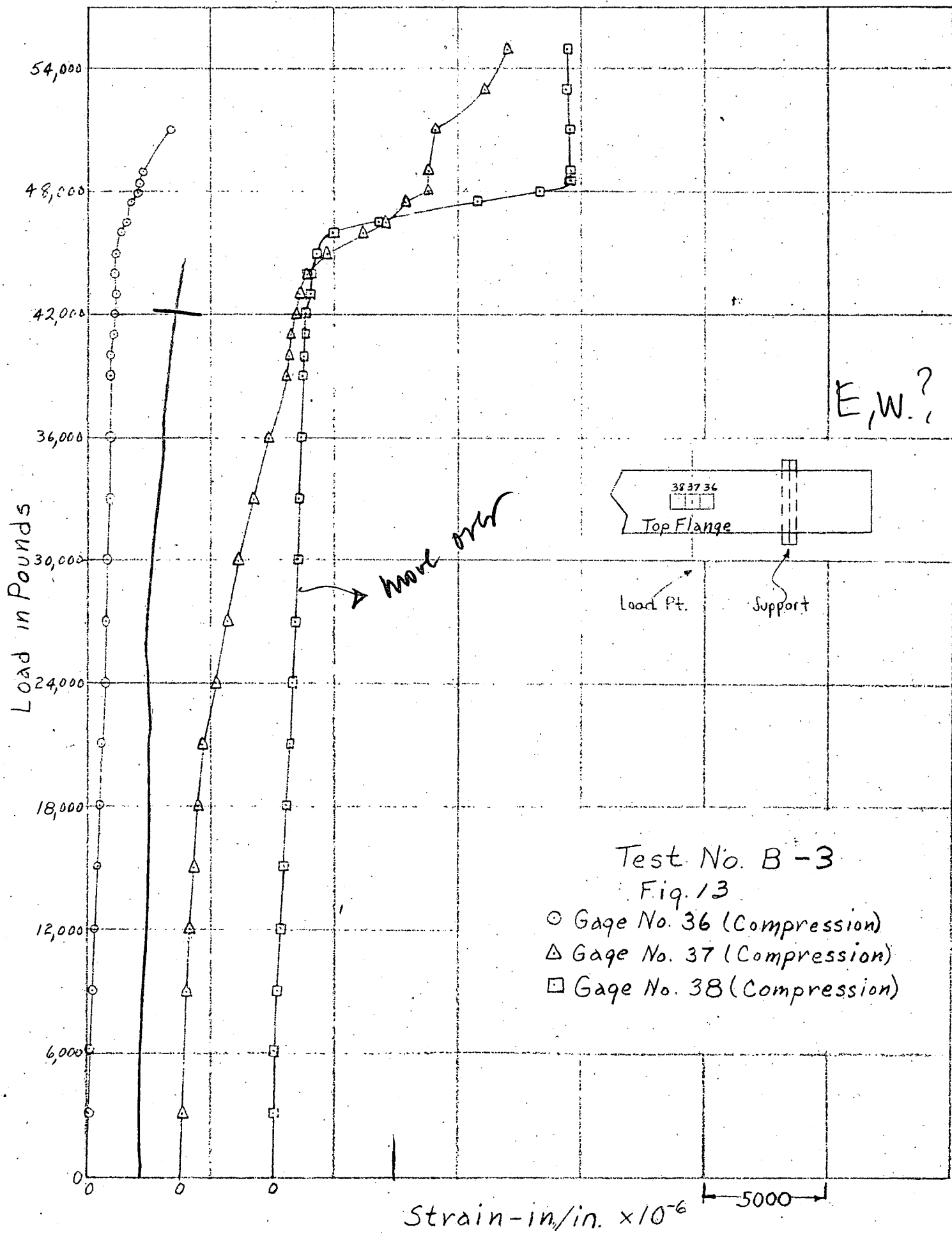


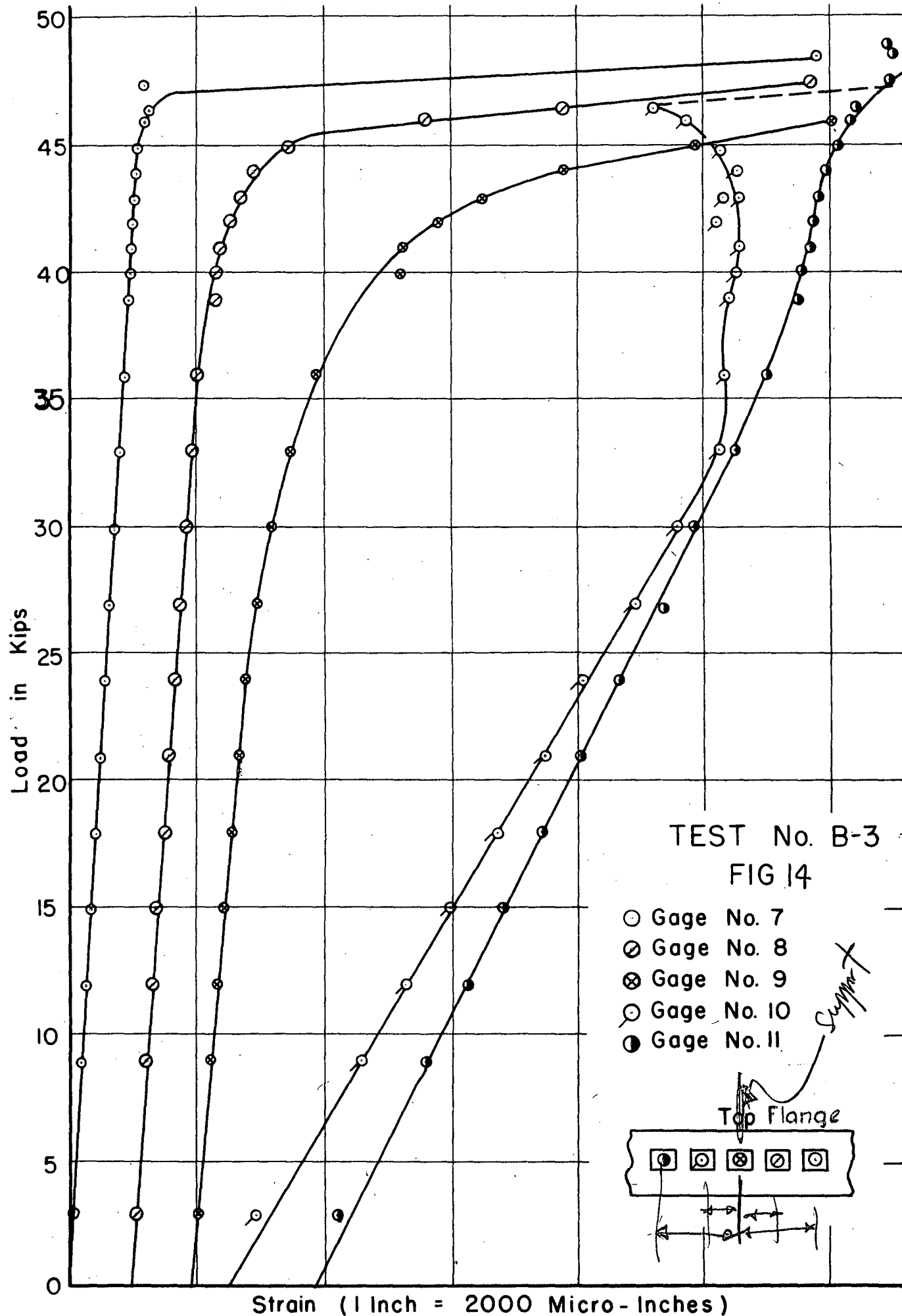
Test B 3  
Fig. 9  
Deflection, Strain & Level  
Gage Locations

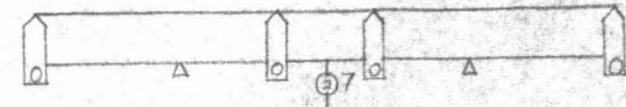
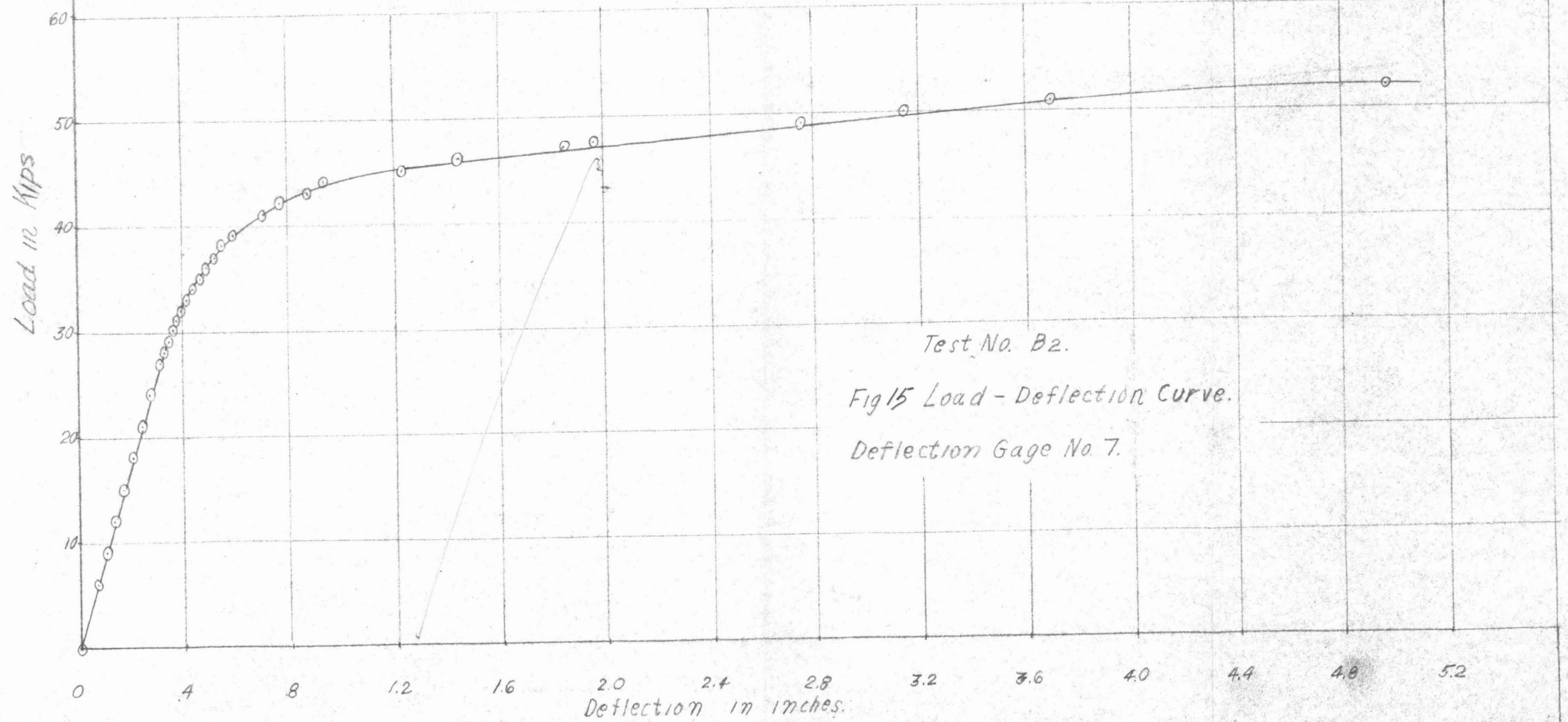




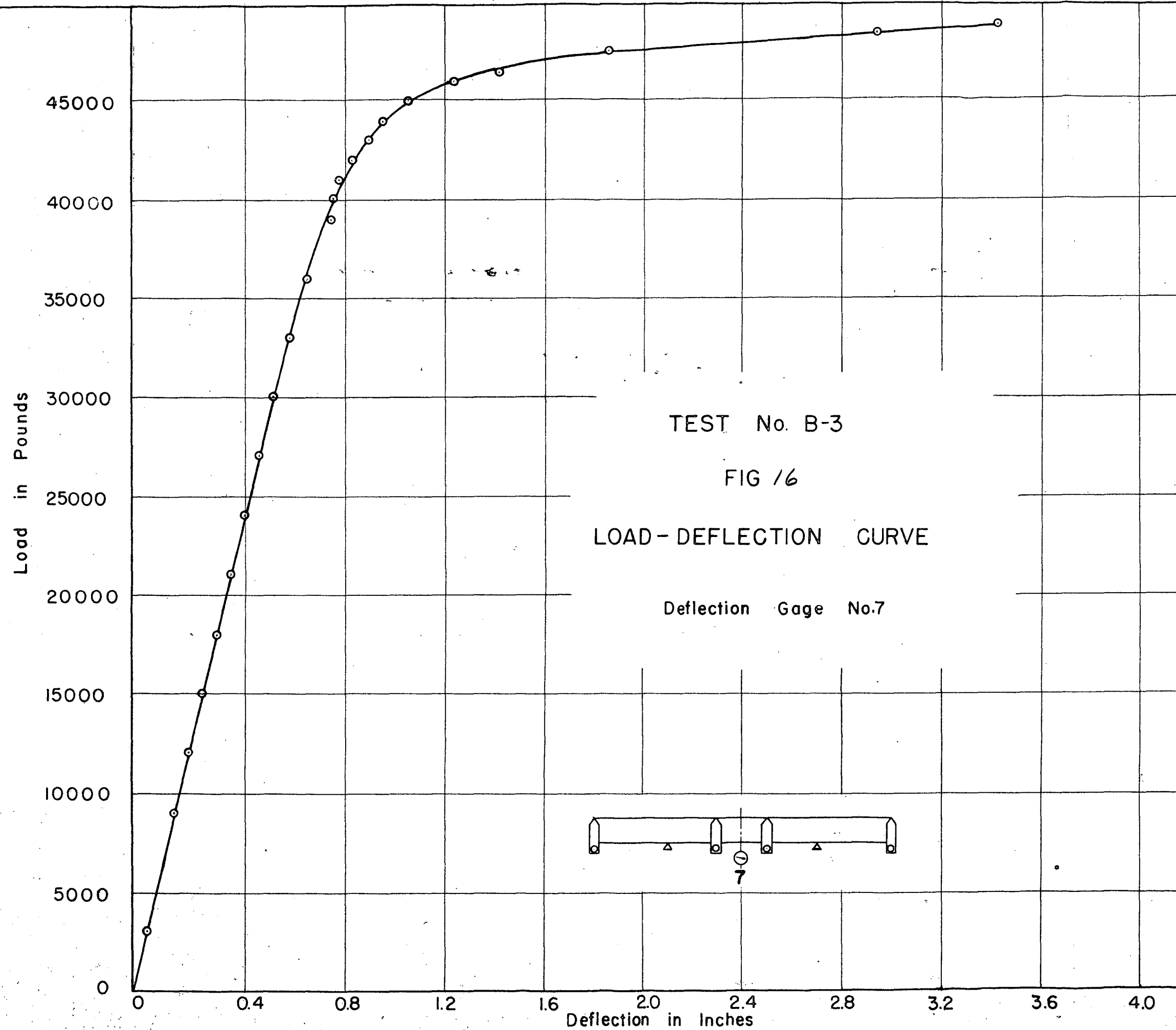




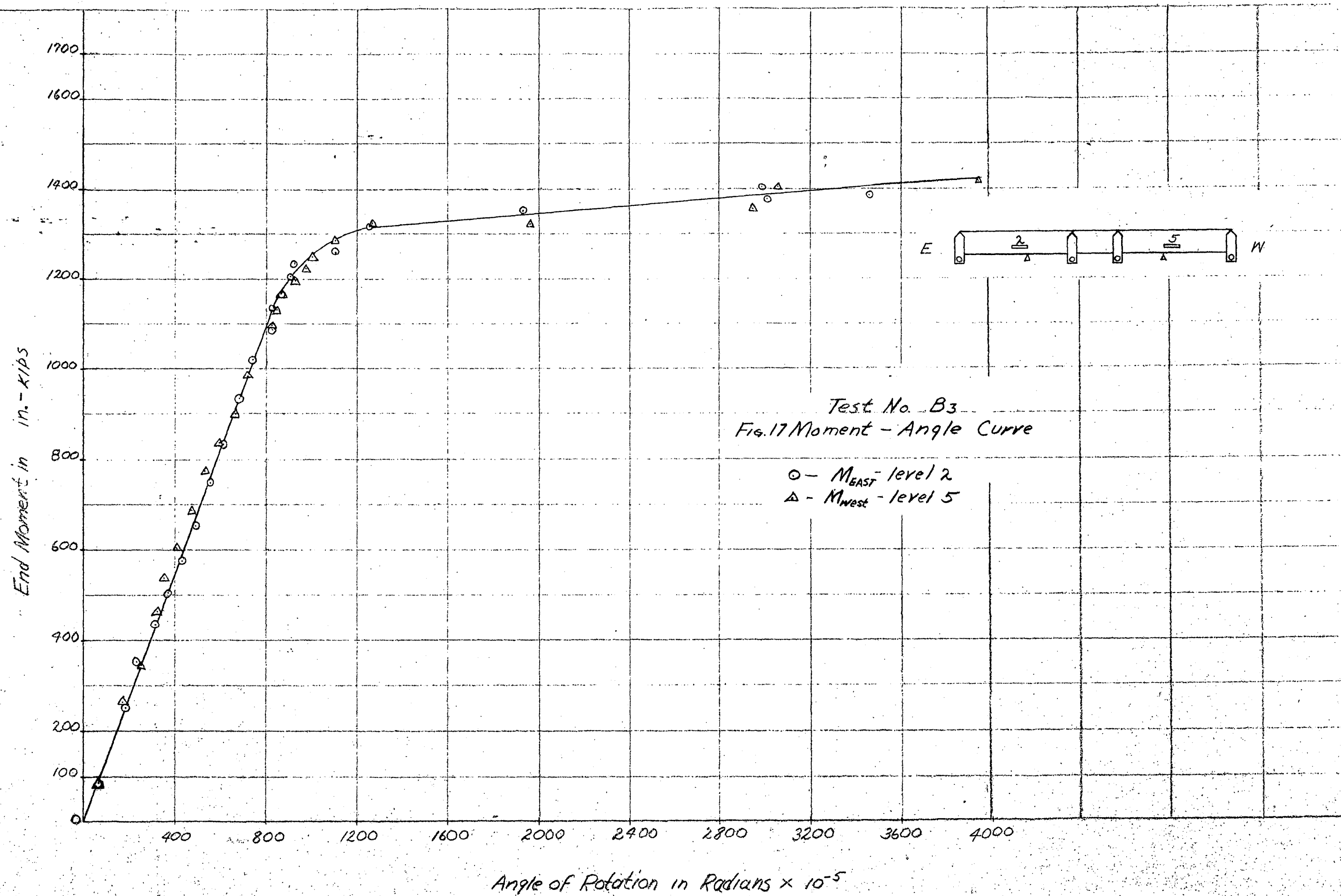




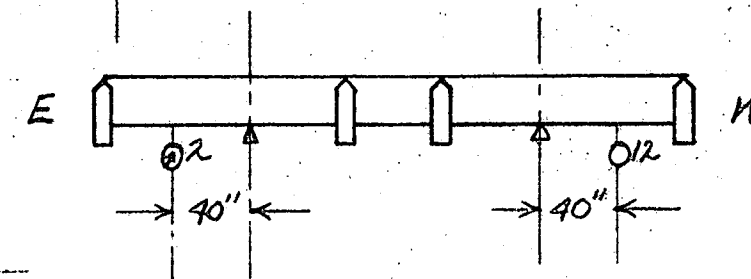
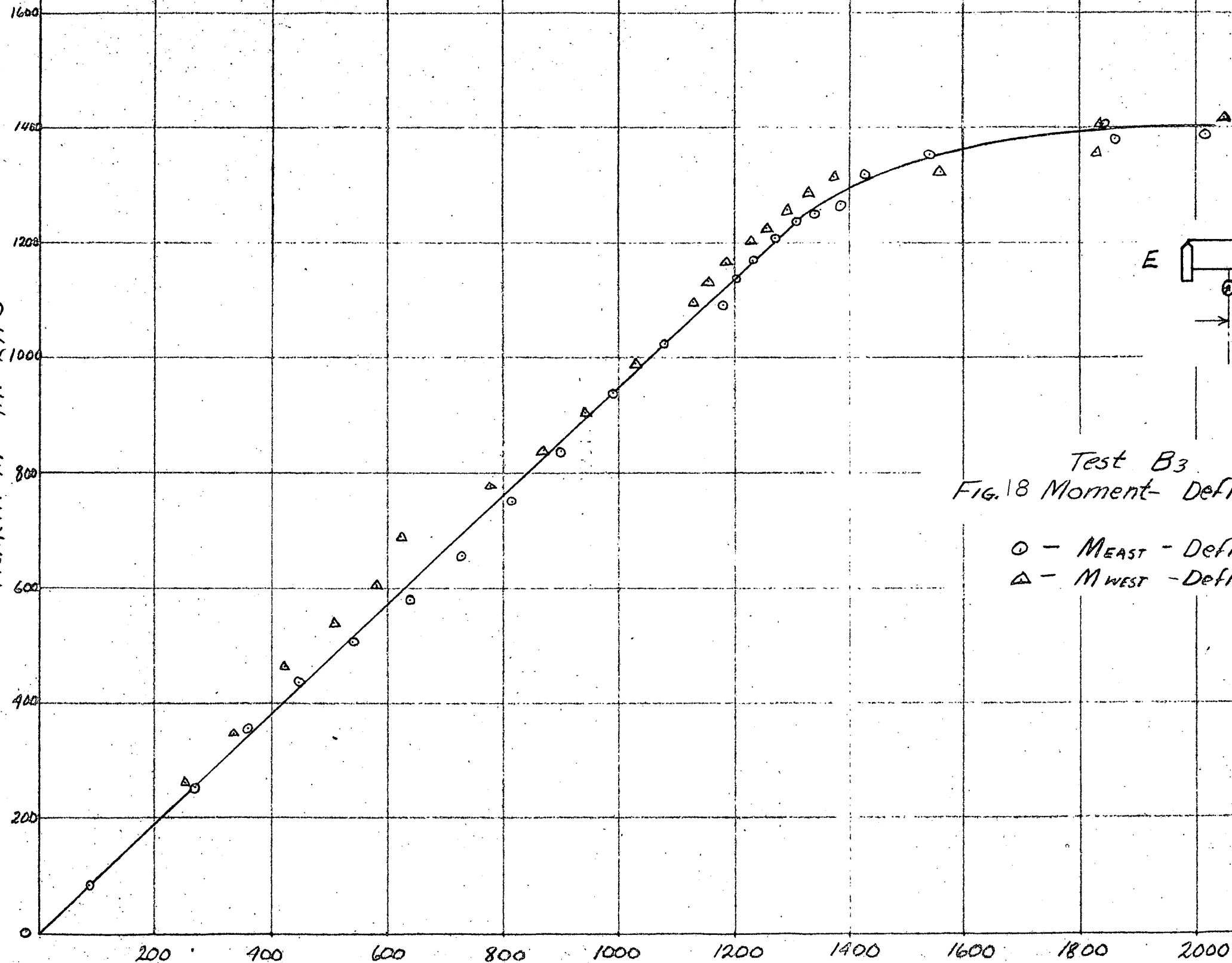








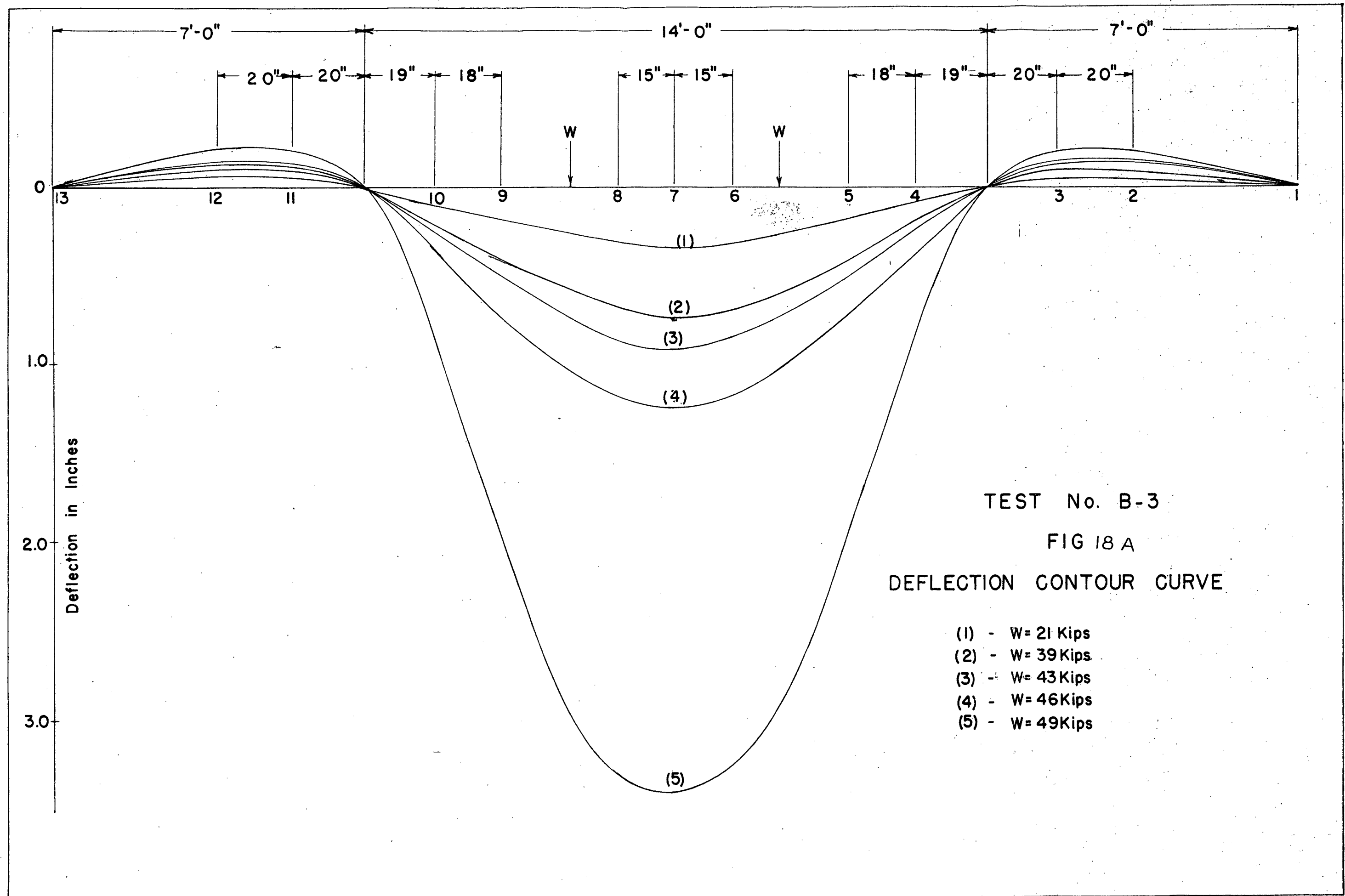
Moment in in.-Kips

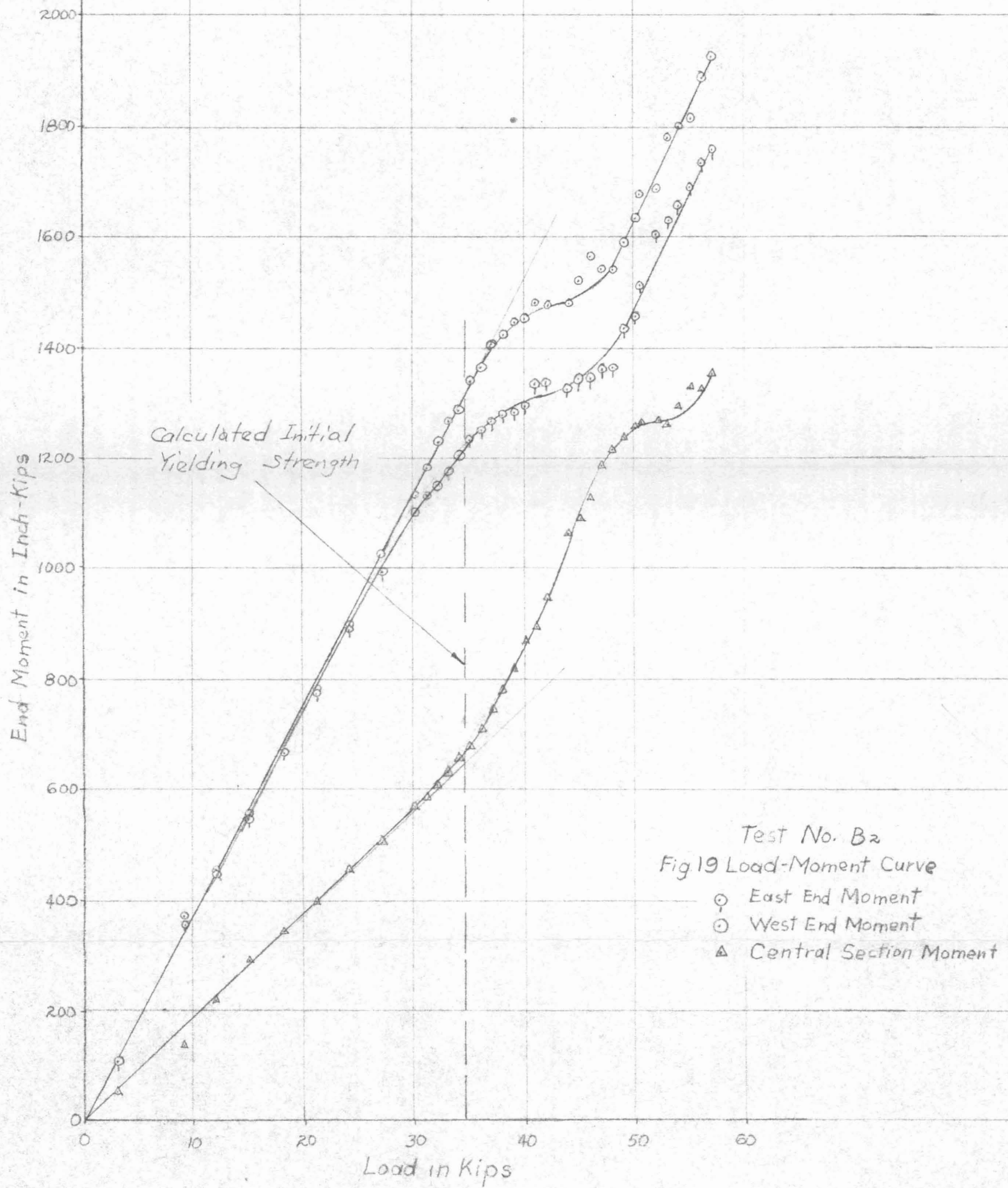
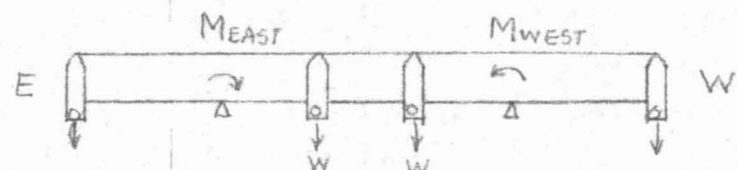


Test B3  
FIG. 18 Moment- Deflection Curve

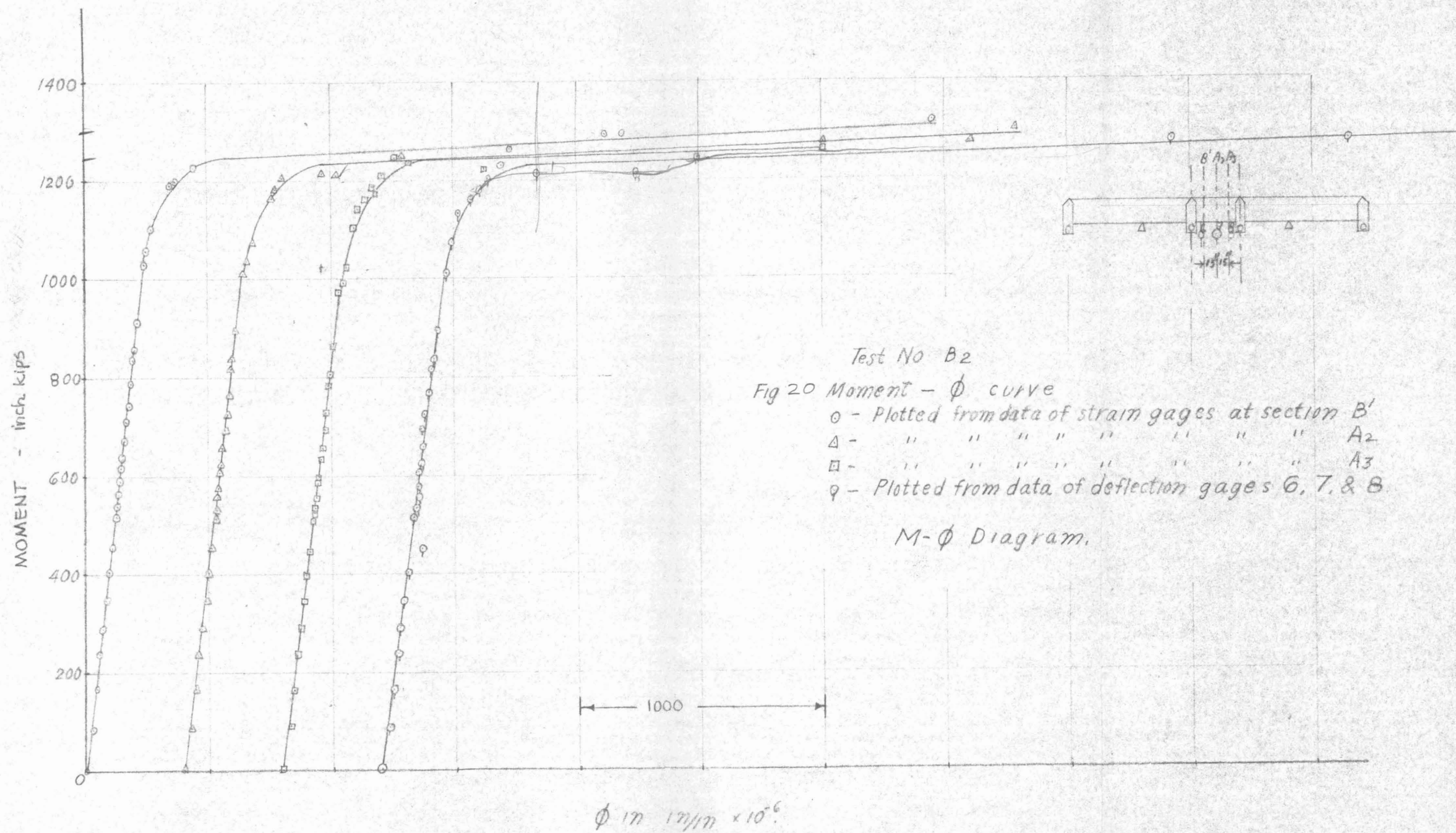
○ -  $M_{EAST}$  - Deflection Gage 2  
△ -  $M_{WEST}$  - Deflection Gage 12

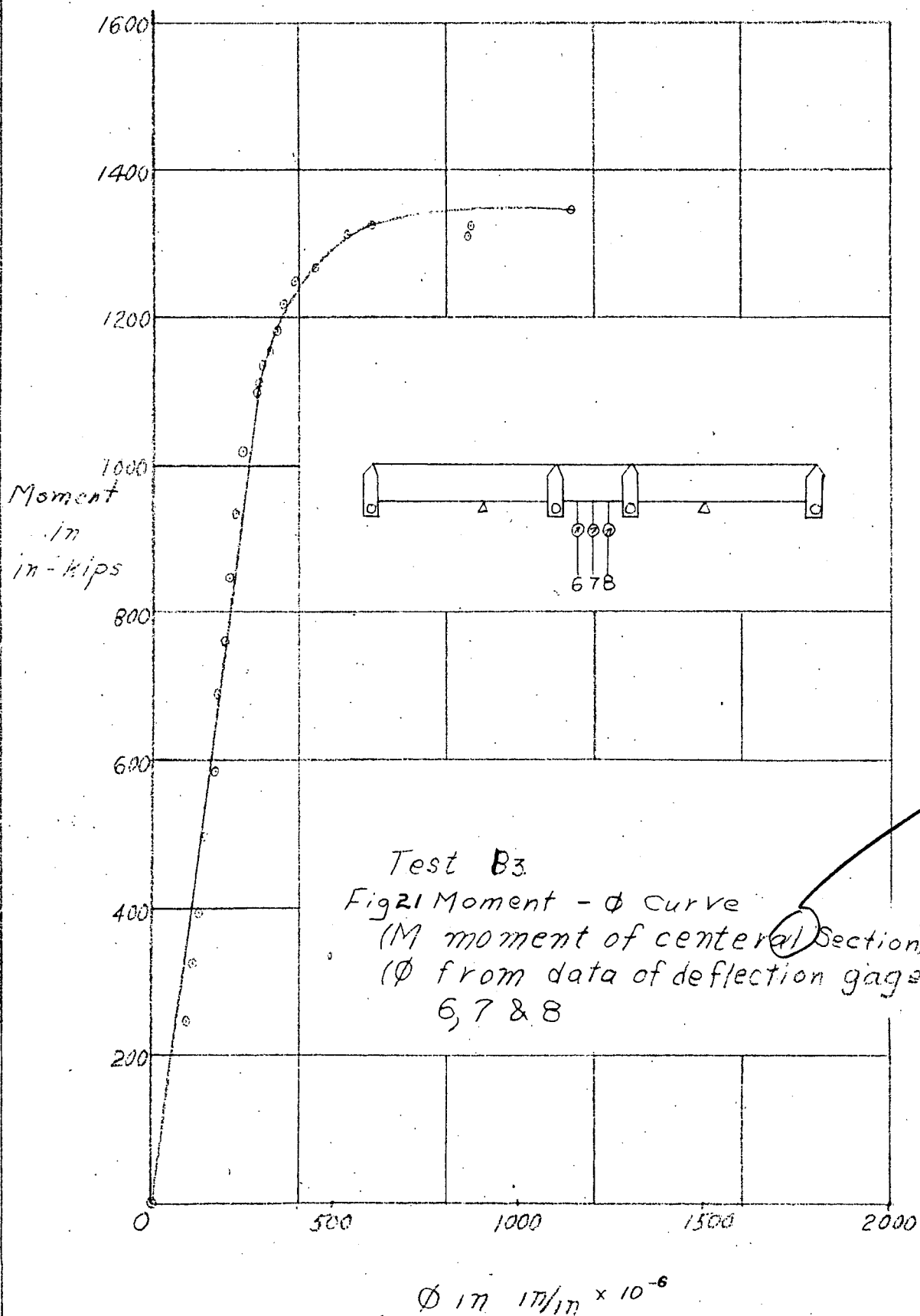
Deflection inches  $\times 10^{-4}$

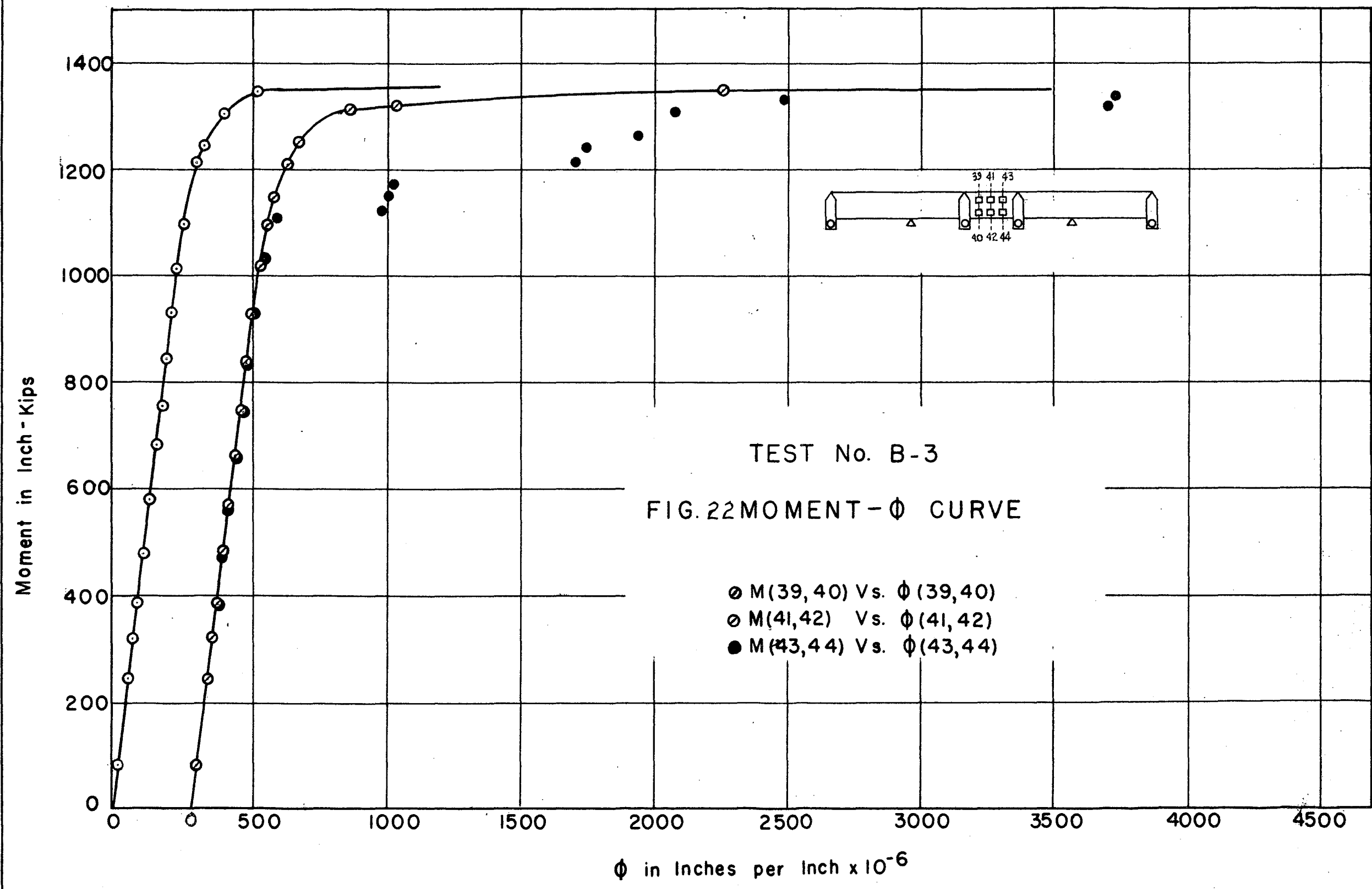




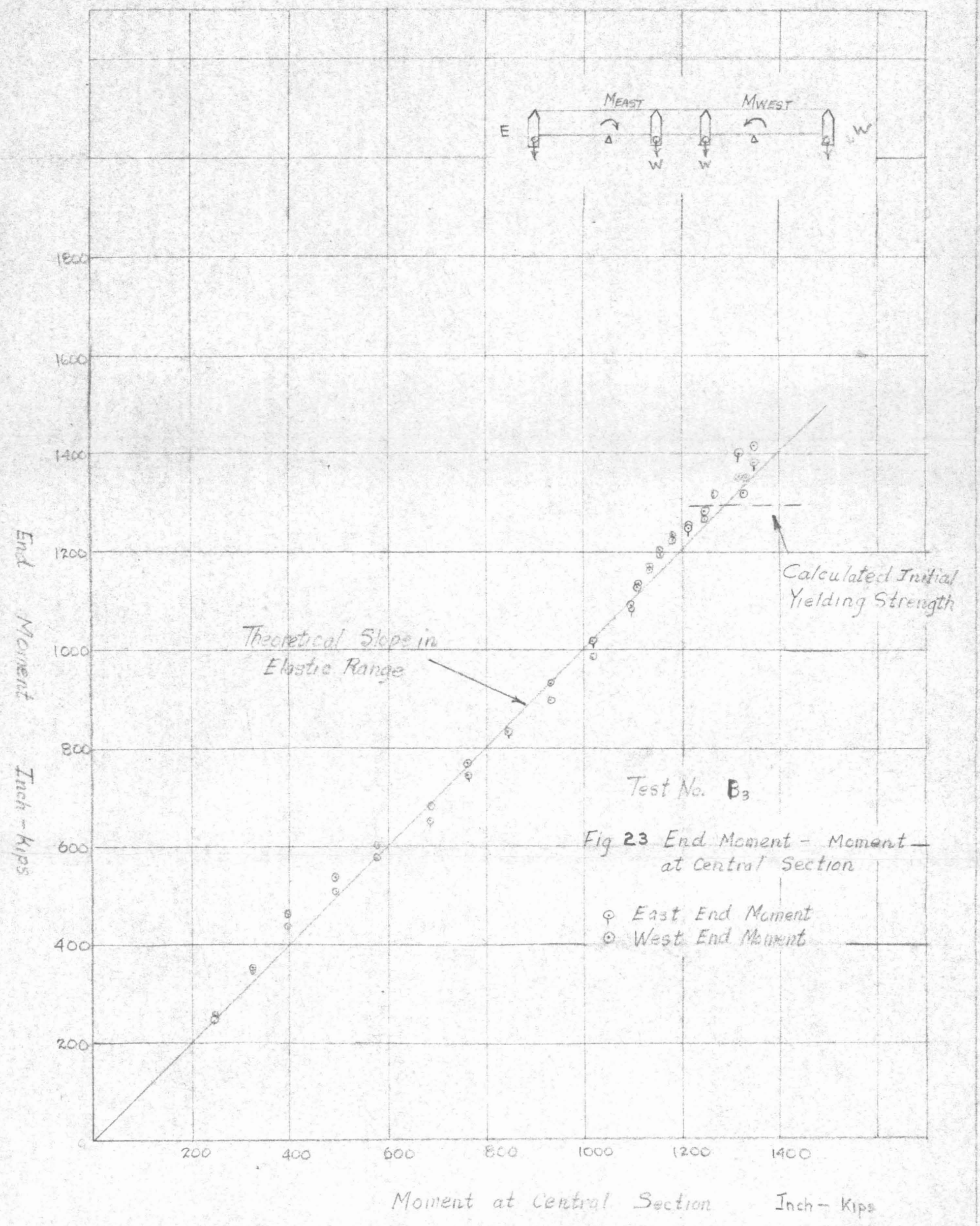
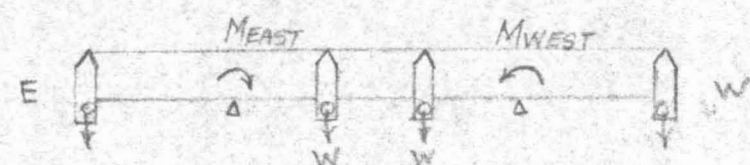














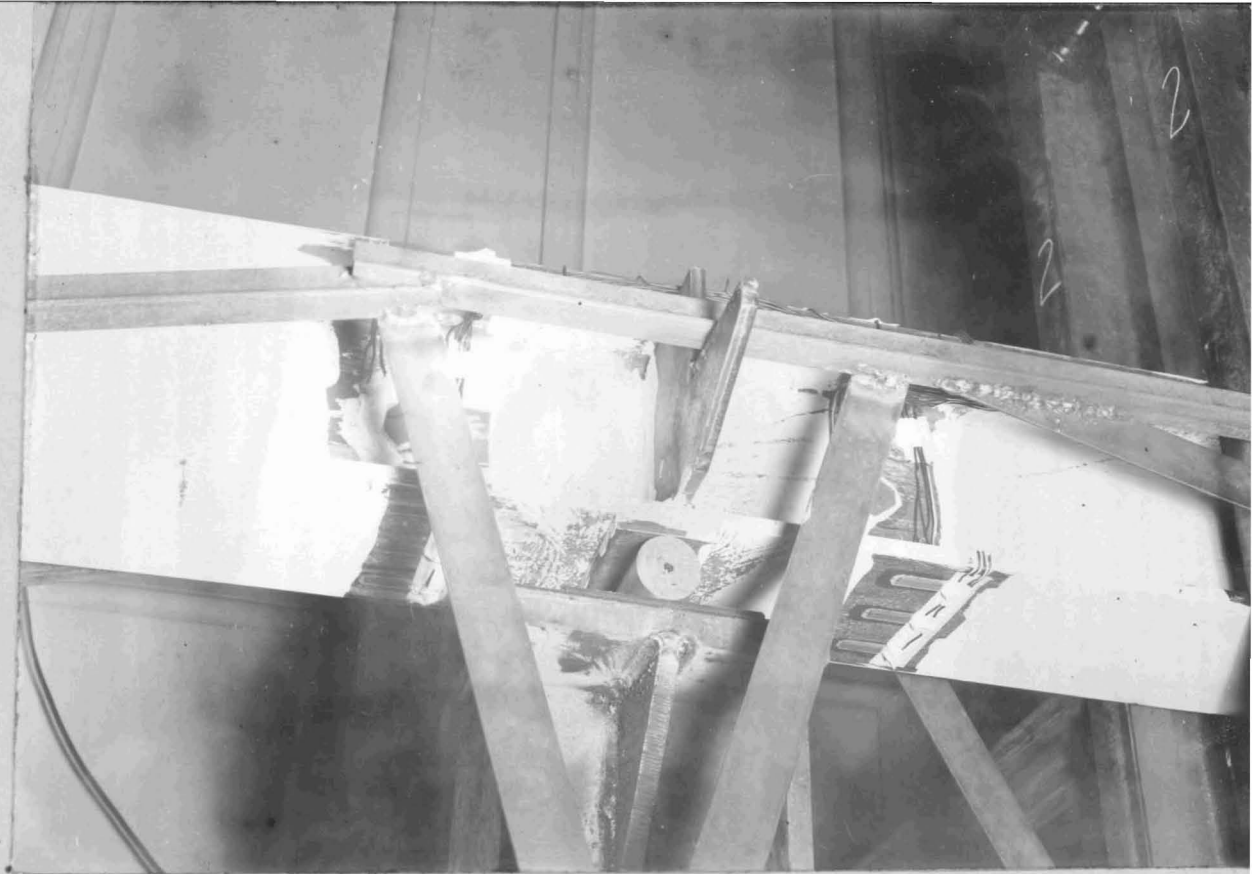
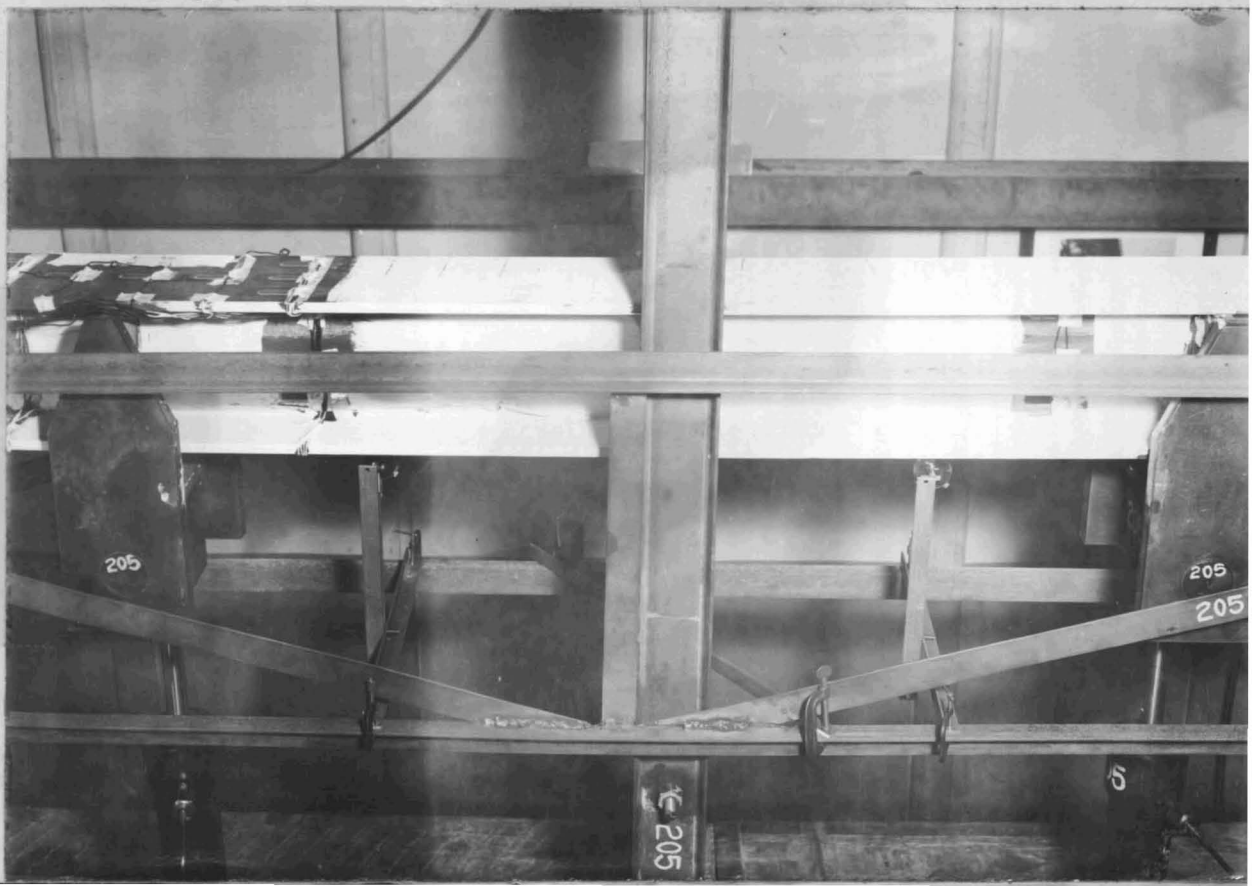


Fig. 24. Lueder lines developed around the support of continuous beam B2 at a load  $W = 44$  kips.

Fig. 25. Flow lines commencing on the top flange of the central span at a load  $W = 46$  kips in continuous beam B2.



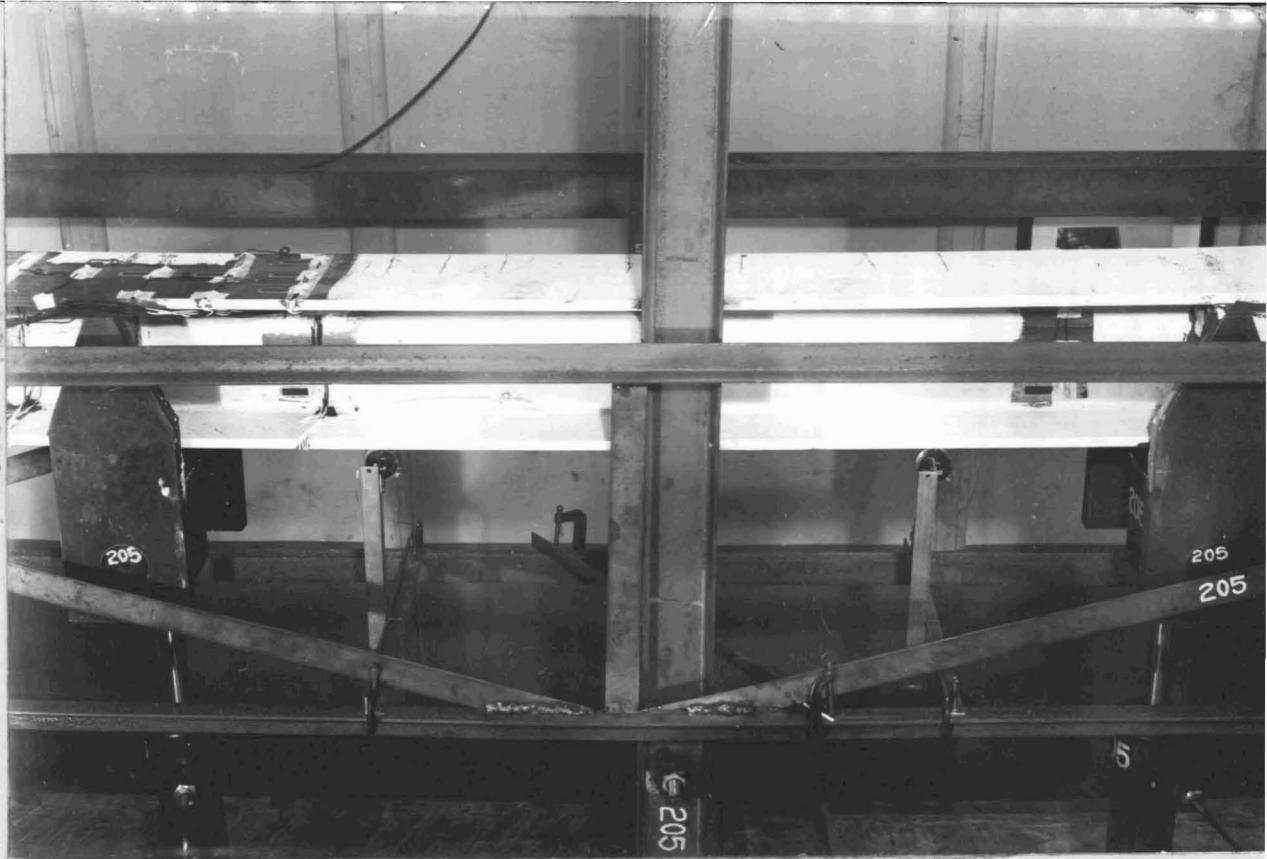


Fig. 26 . The progression of Lueder lines on the top flange of the central span at a load  $W = 47$  kips in continuous beam test B2.

Fig. 27. Lueder lines appearing on the lower flange of the central span at a load  $W = 50.5$  kips, test B2.

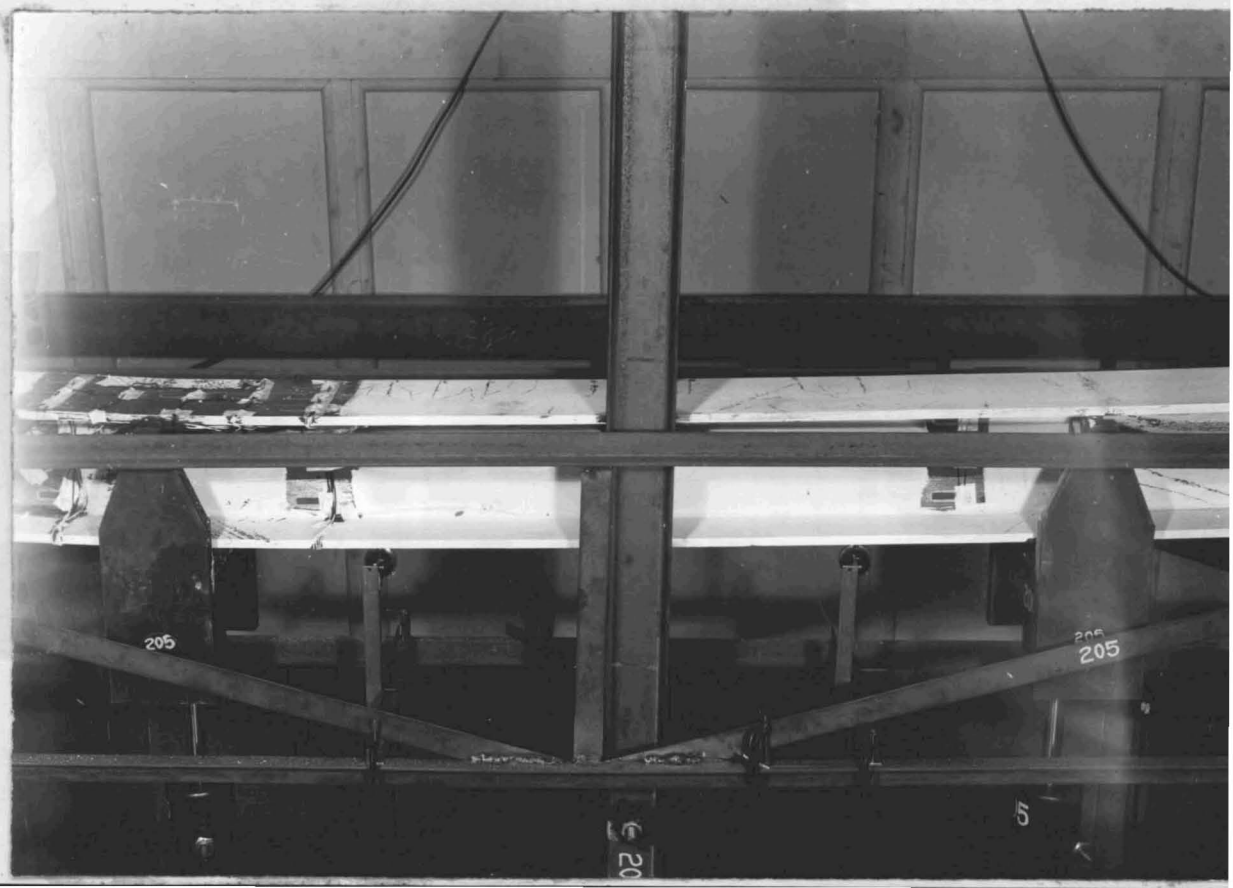
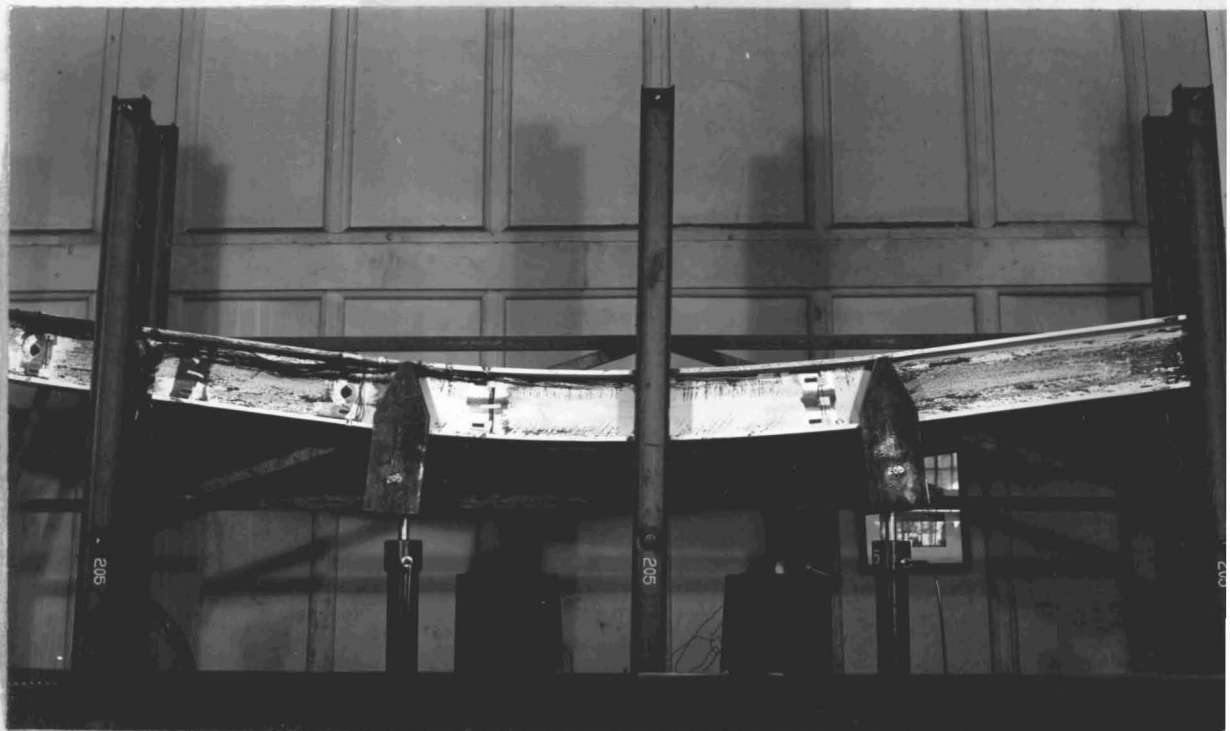
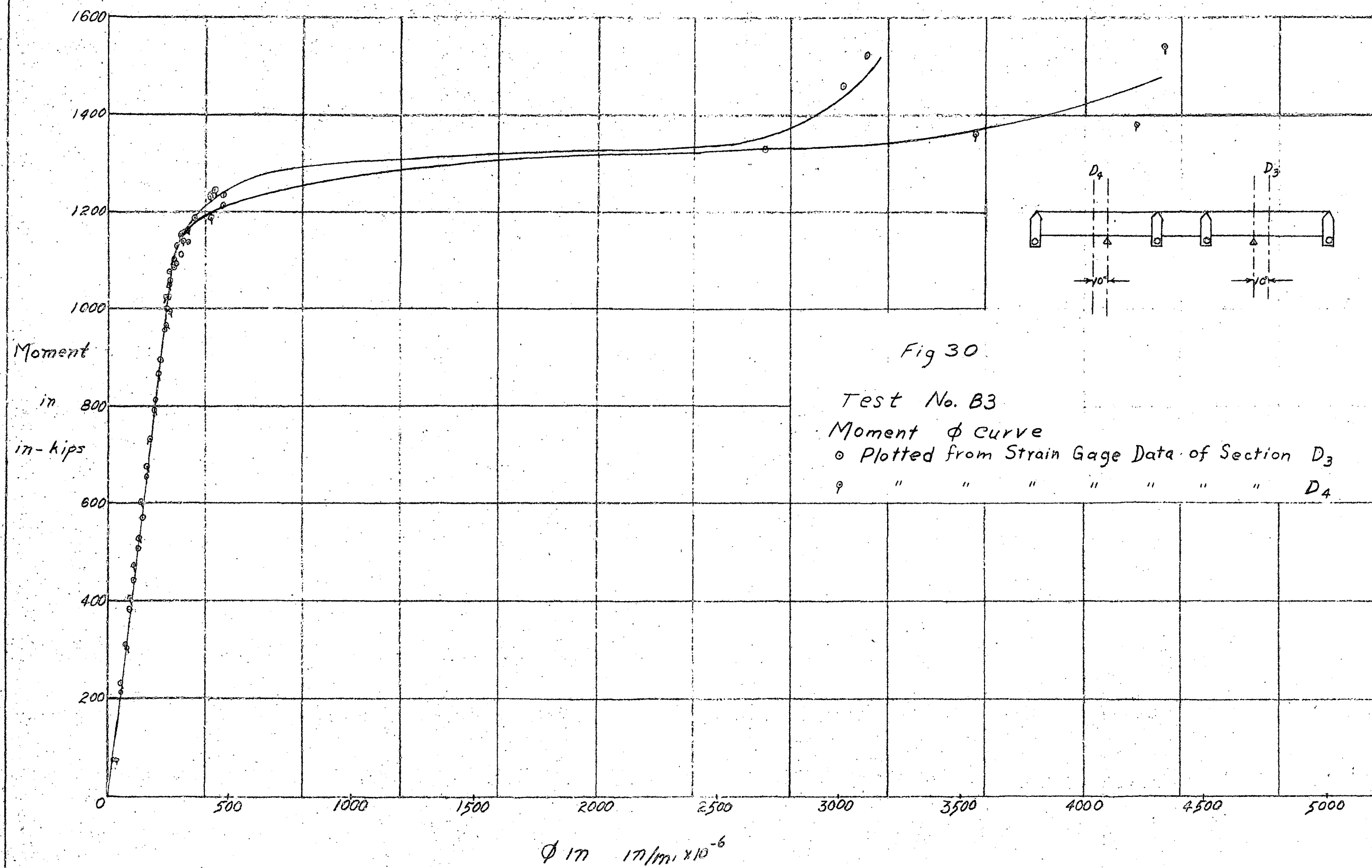




Fig. 28 . The progression of Lueder lines in the lower flange of the central span at a load  $W = 54$  kips in continuous beam test B2.

Fig. 29 . Side view of central span, continuous beam B2 after test.







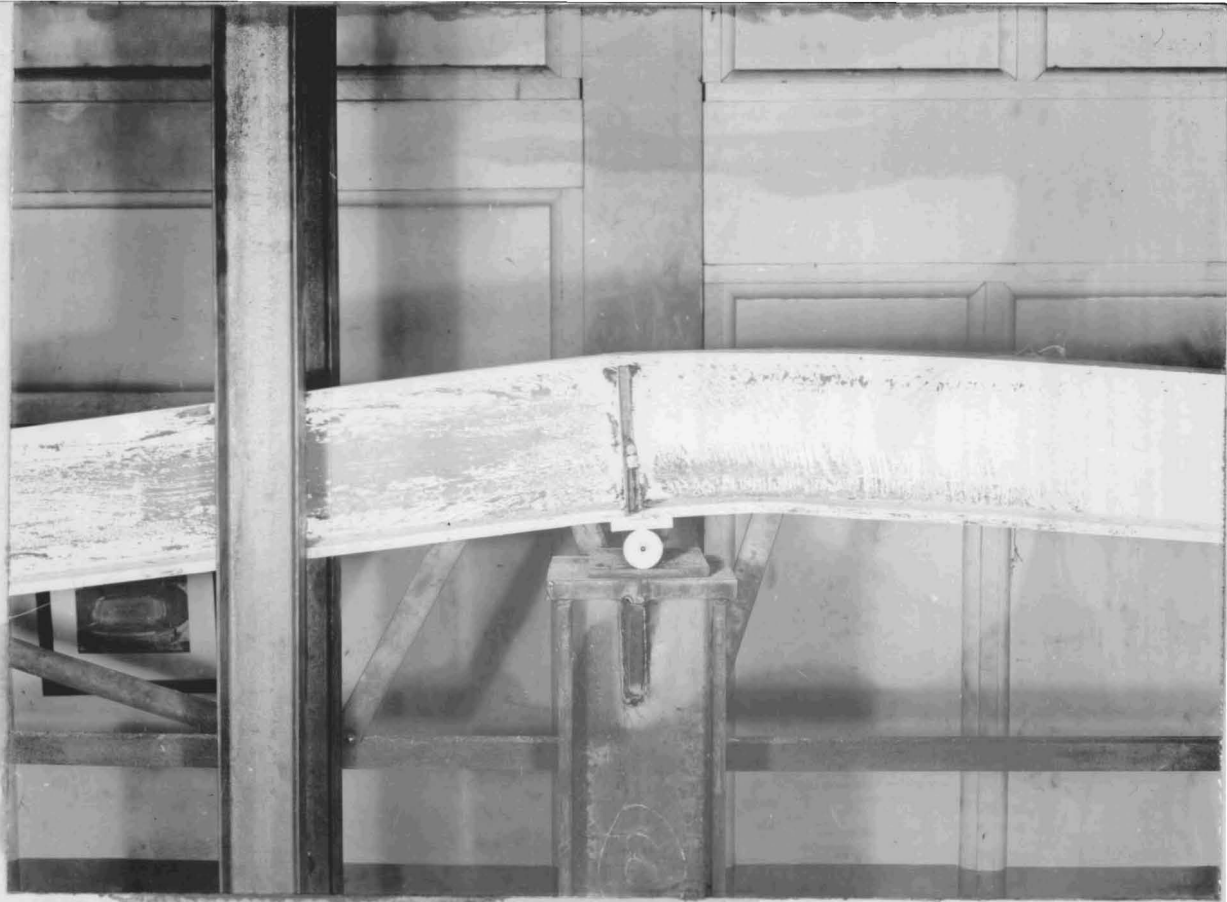
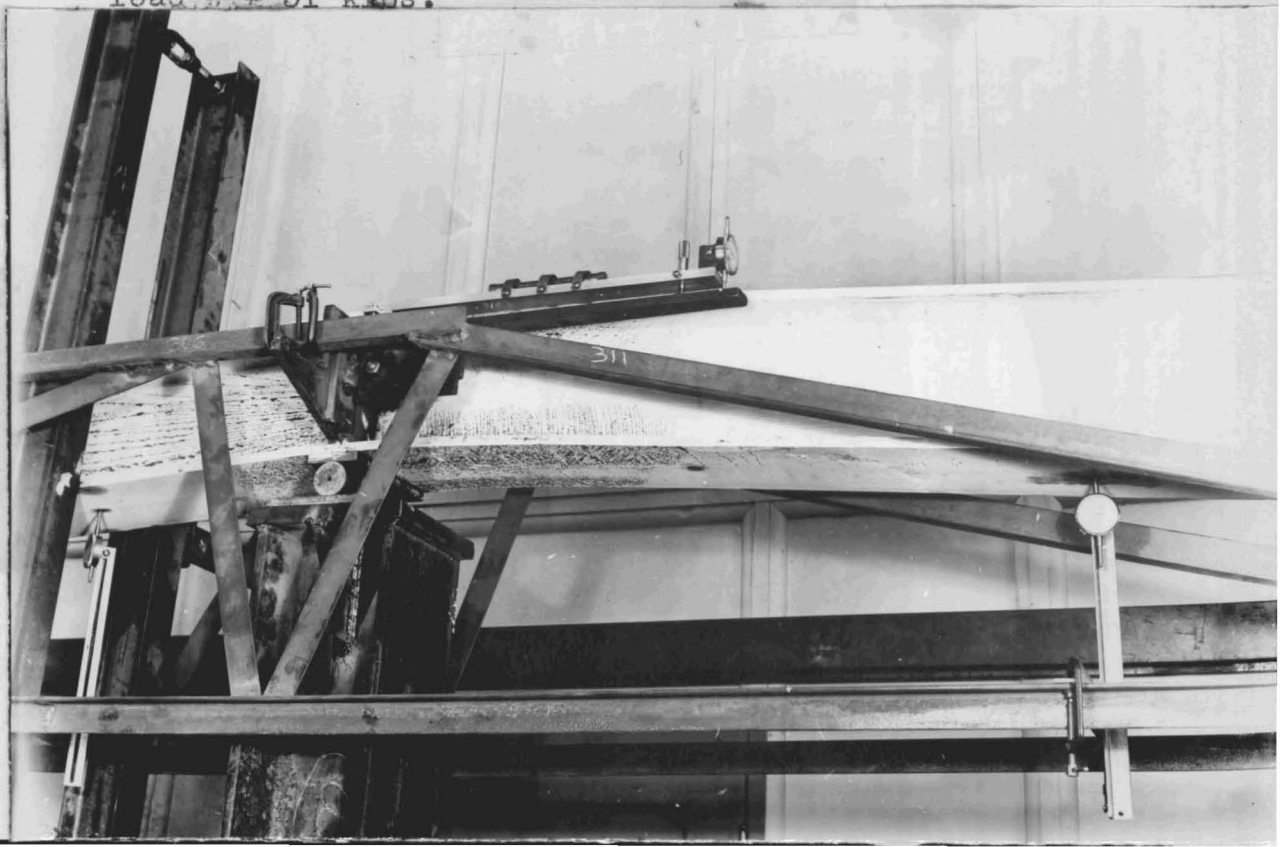
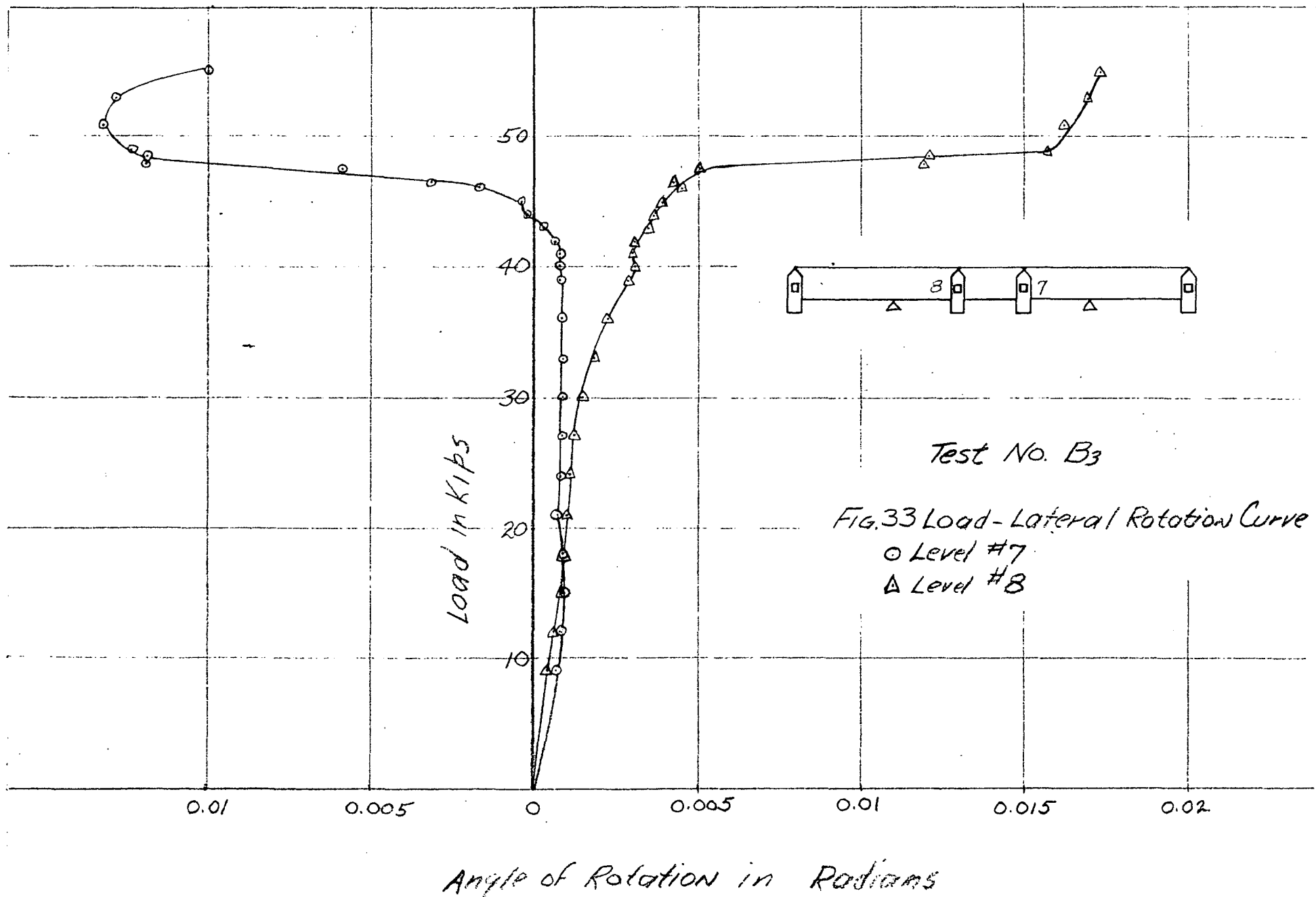


Fig.31 . Local buckling of lower flange near the support in continuous beam B2.

Fig.32 . Lueder line patterns in the cantilever portion of . continuous beam B3 showing the penetration of plastic zone into the web at a load  $W = 51$  kips.





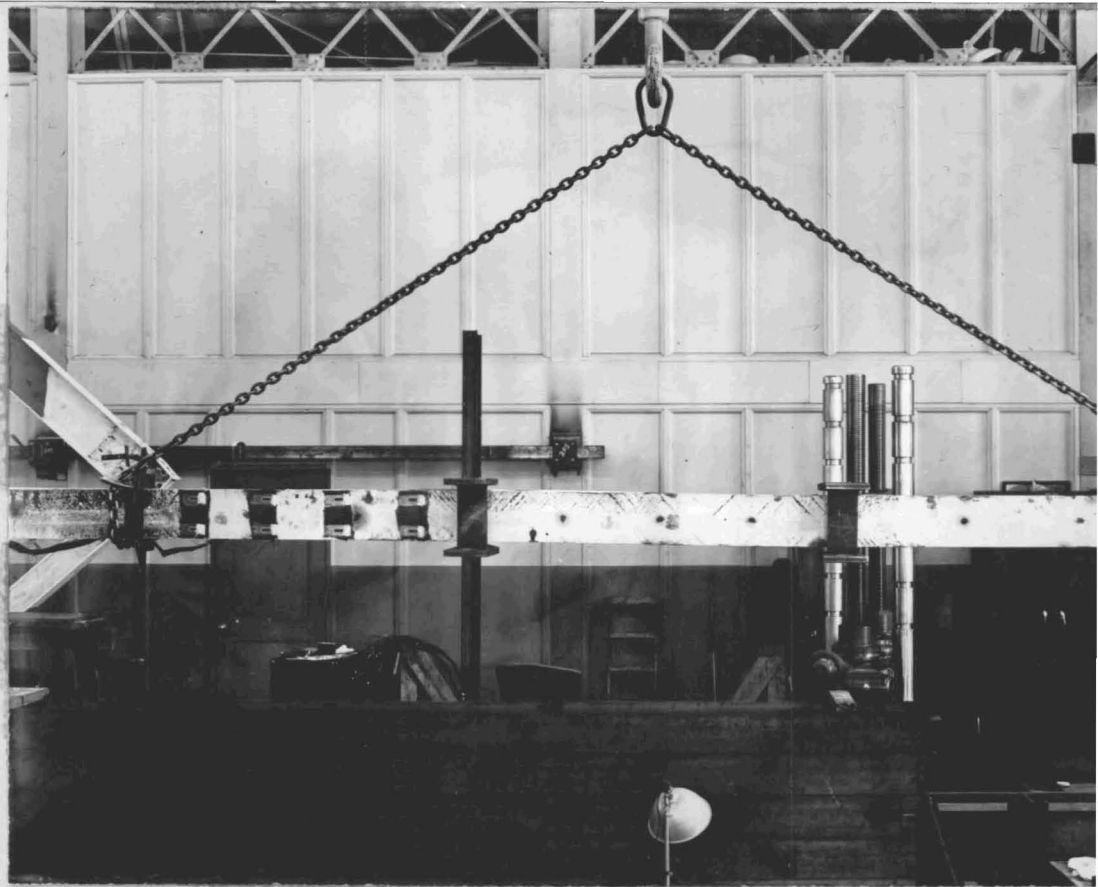


Fig. 34. Continuous beam B2 twisted after test due to lateral buckling.

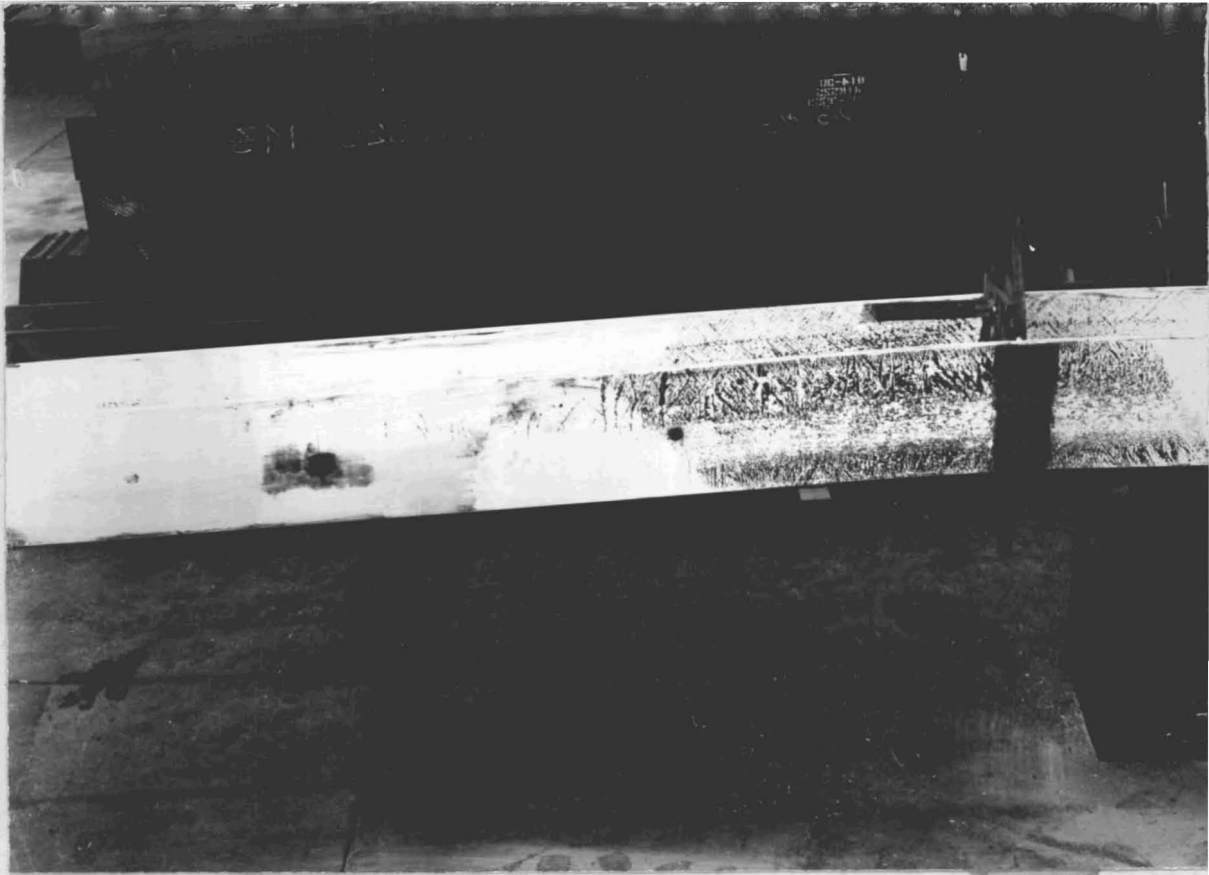


Fig.34A. Lueder line pattern near the support of continuous beam B3 showing torsional stress developed due to lateral buckling.



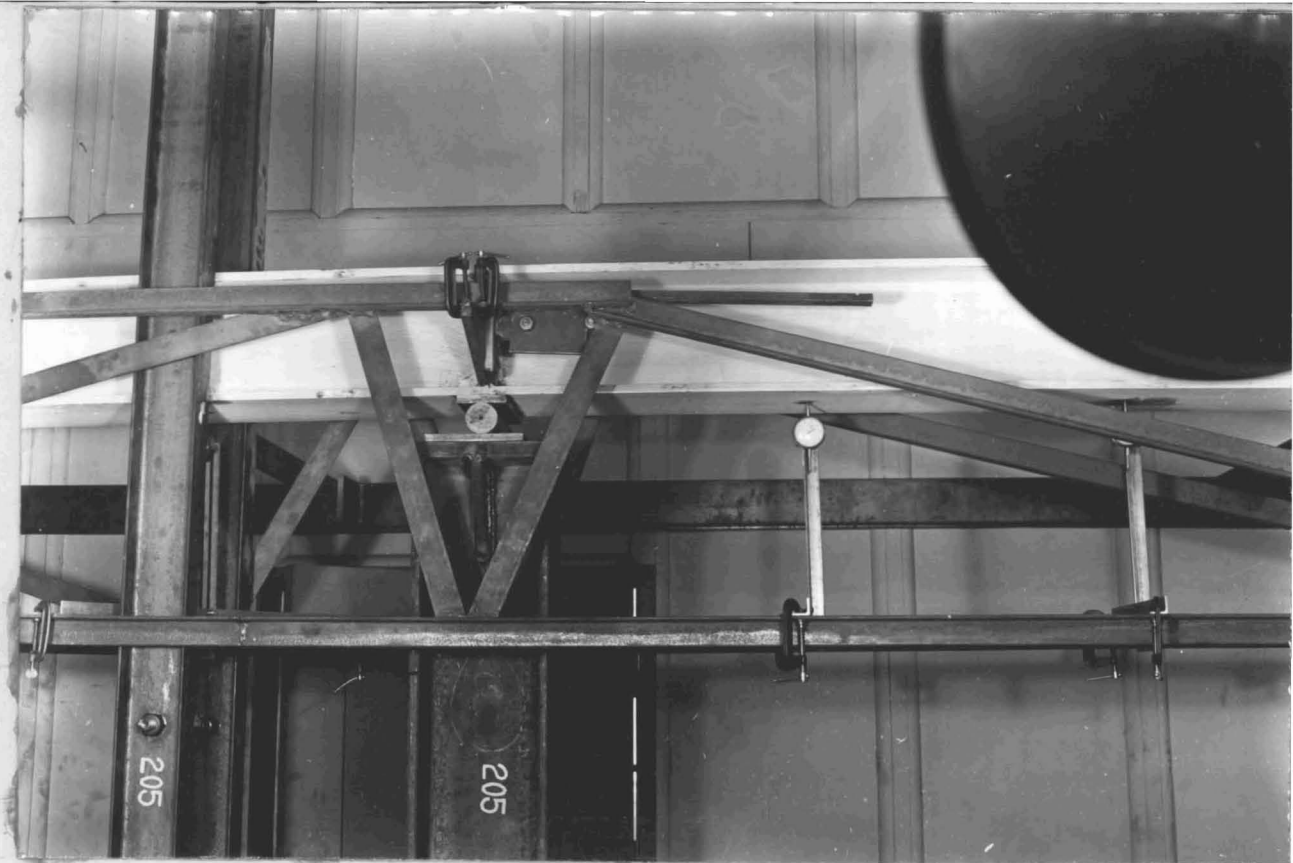
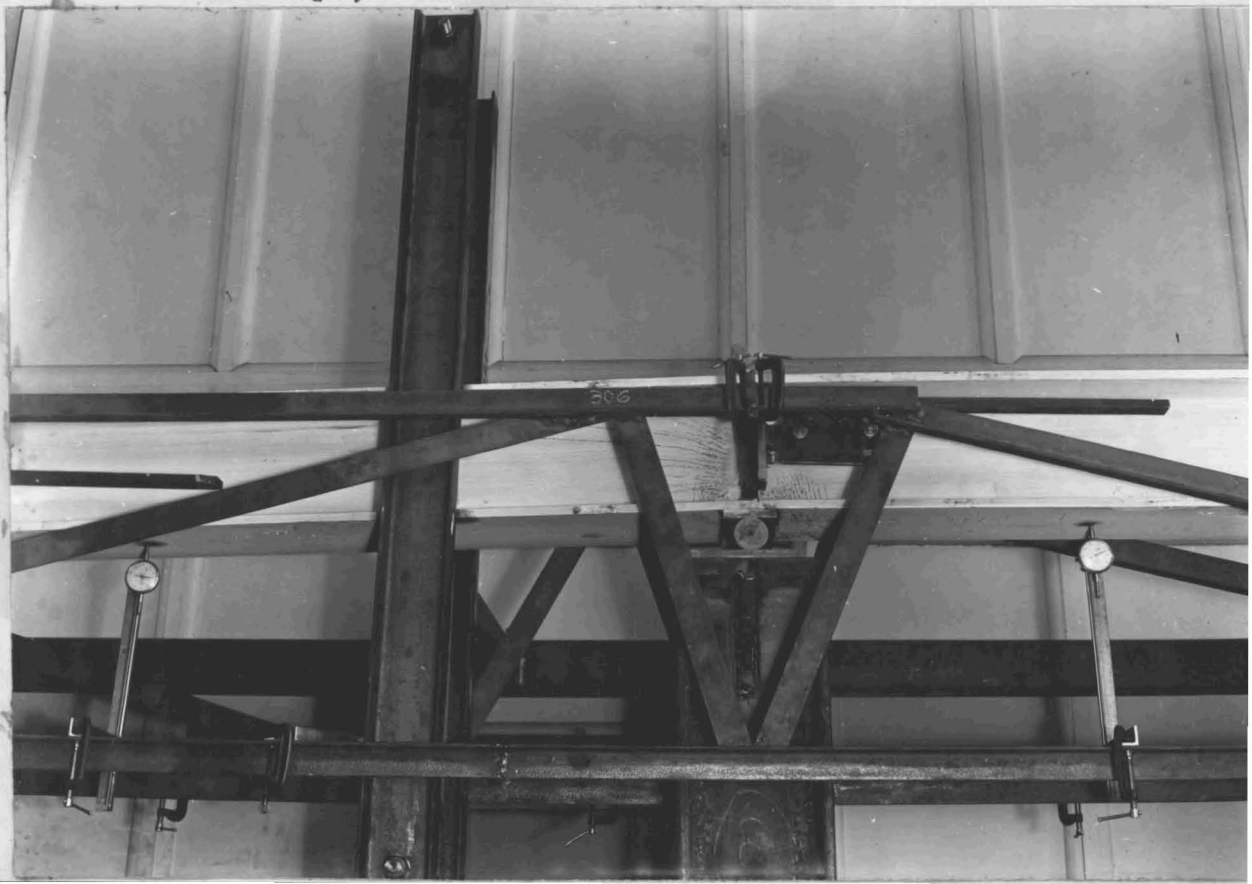


Fig. 35. Lines developed by local shear failure in web near the support at a load  $W = 39$  kips. Continuous beam test B3.

Fig. 36. Progression of shear yielding in the web.  $W = 47.5$  kips, test B3.



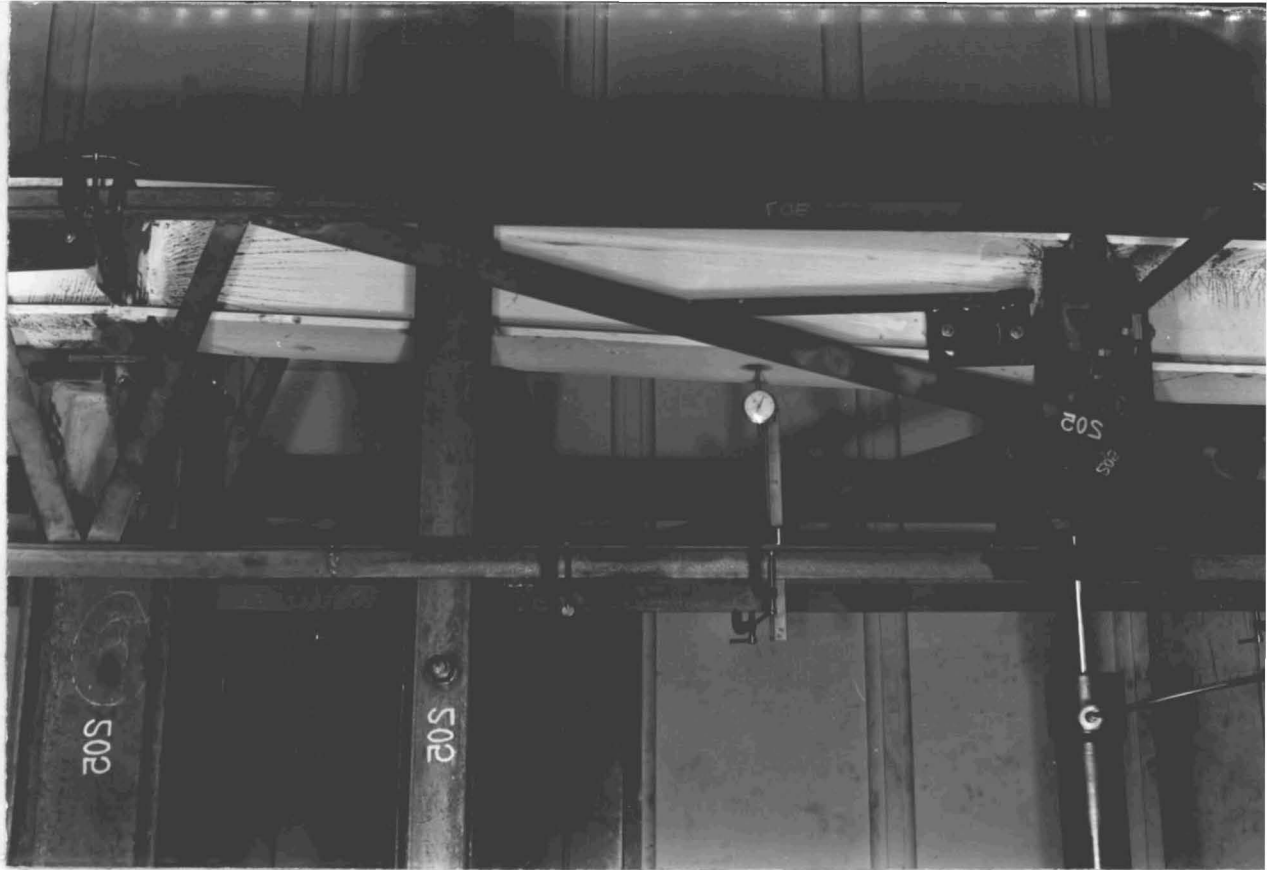
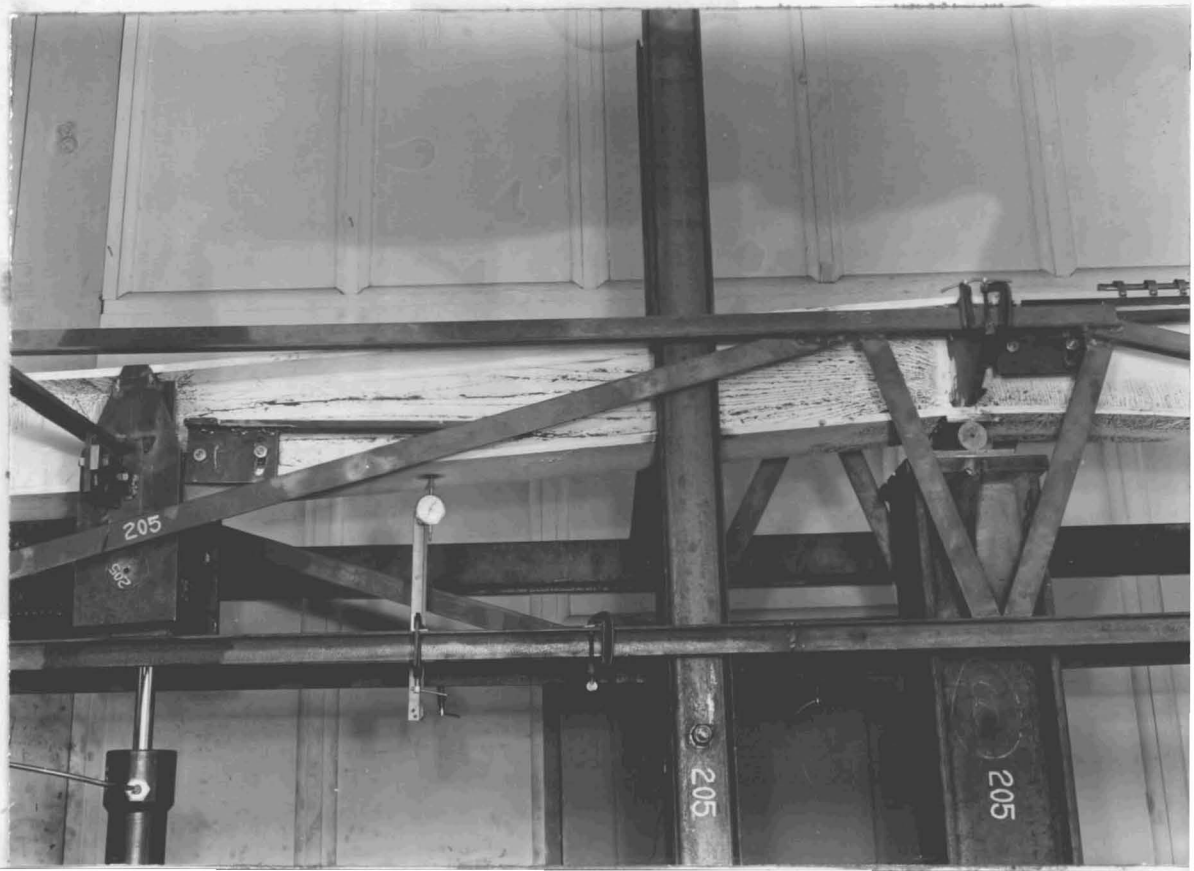


Fig. 37 . Progression of Lueder lines developed in the web by shear failure at a load  $W = 48$  kips. Test B3.

Fig. 38 . Shear pattern of continuous beam B3.  
 $W = 51$  kips.



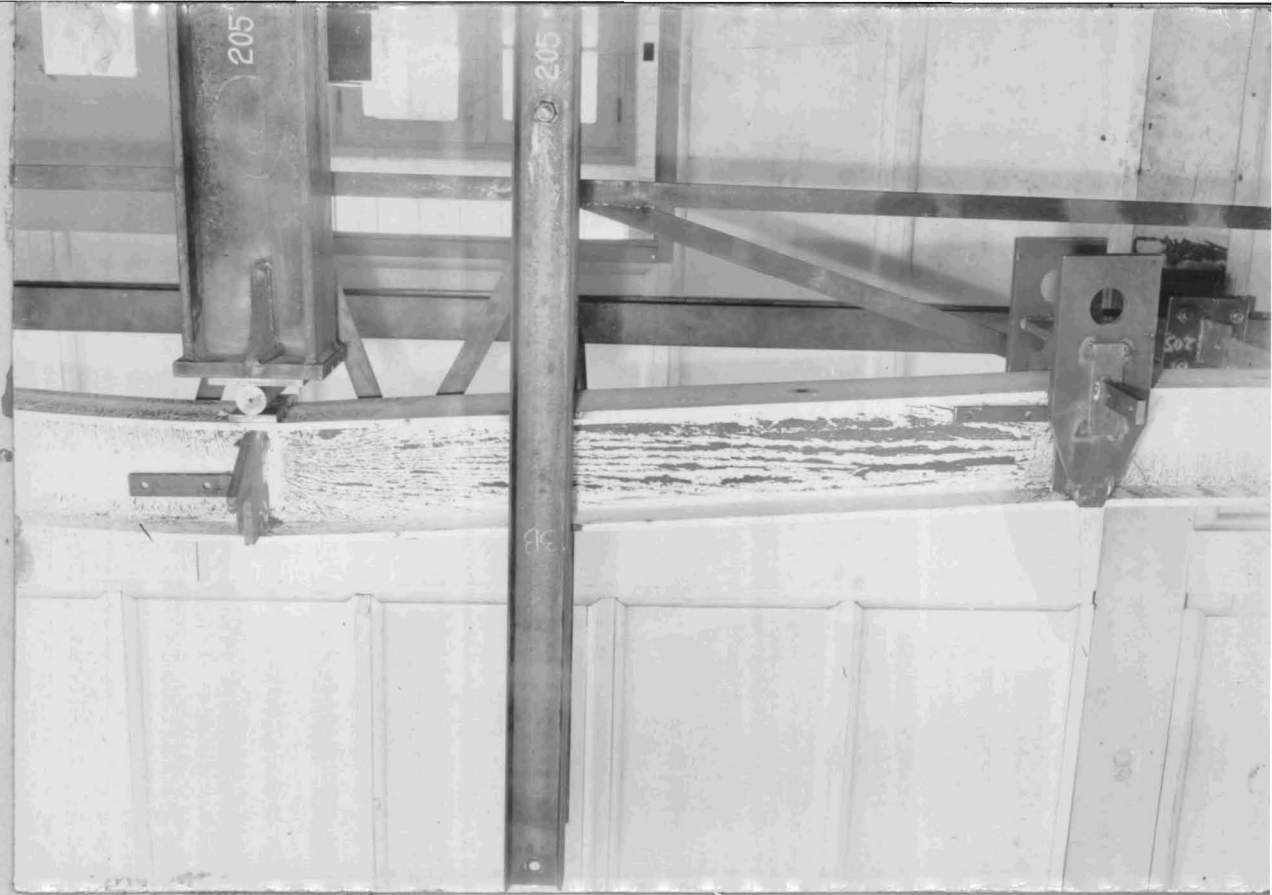
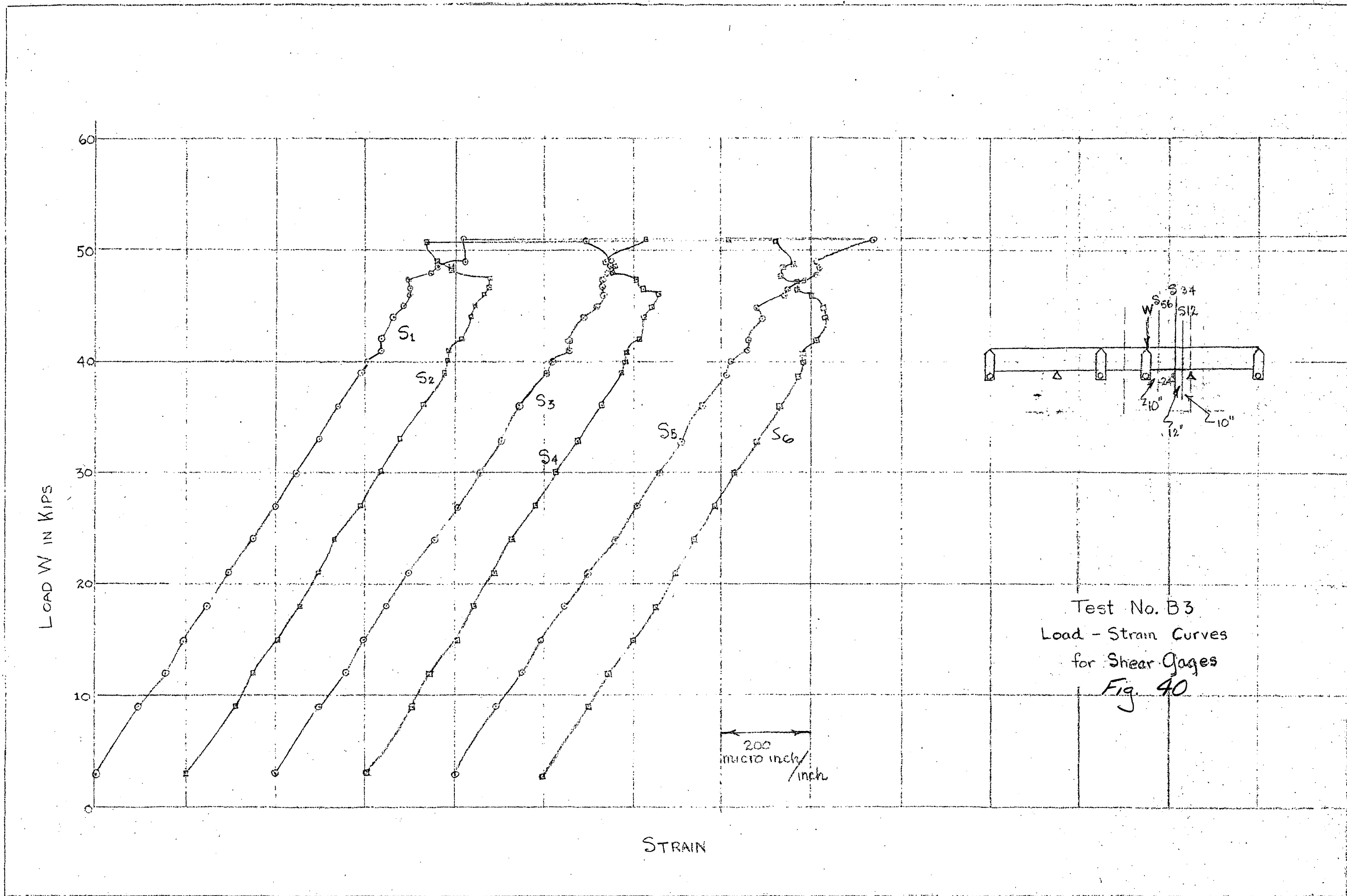
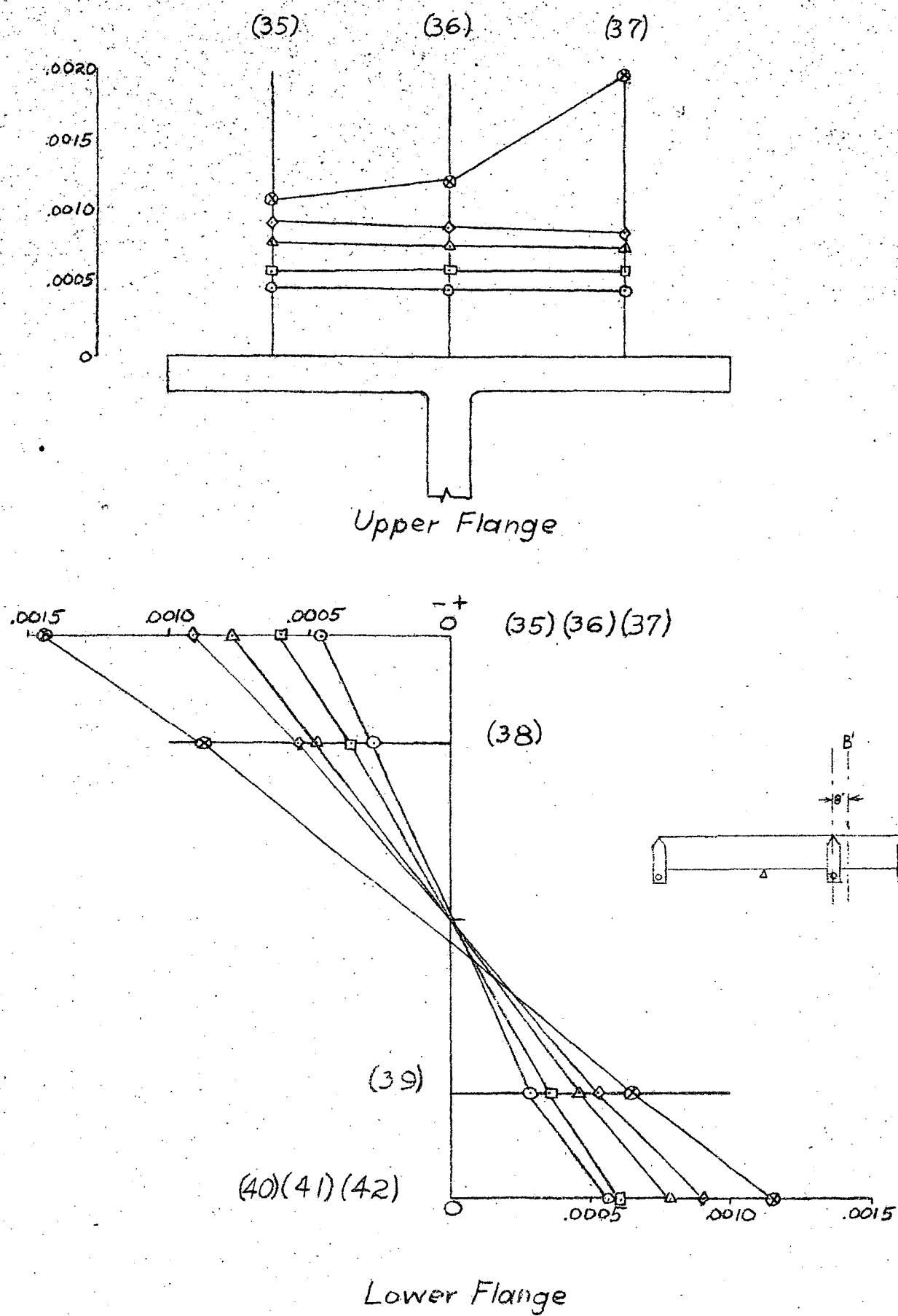


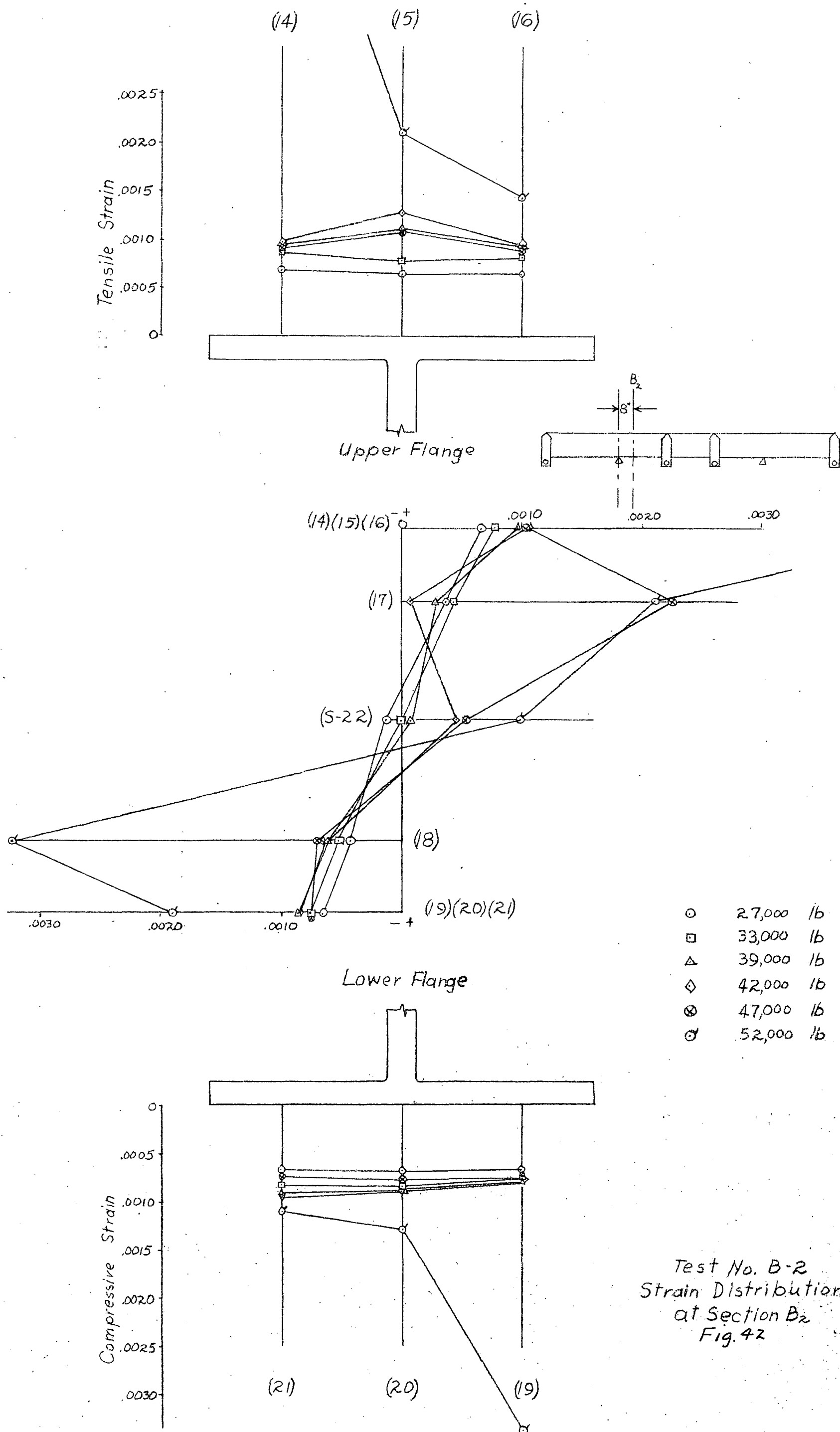
Fig.39. Lueder line pattern of continuous beam  
B3 after test.



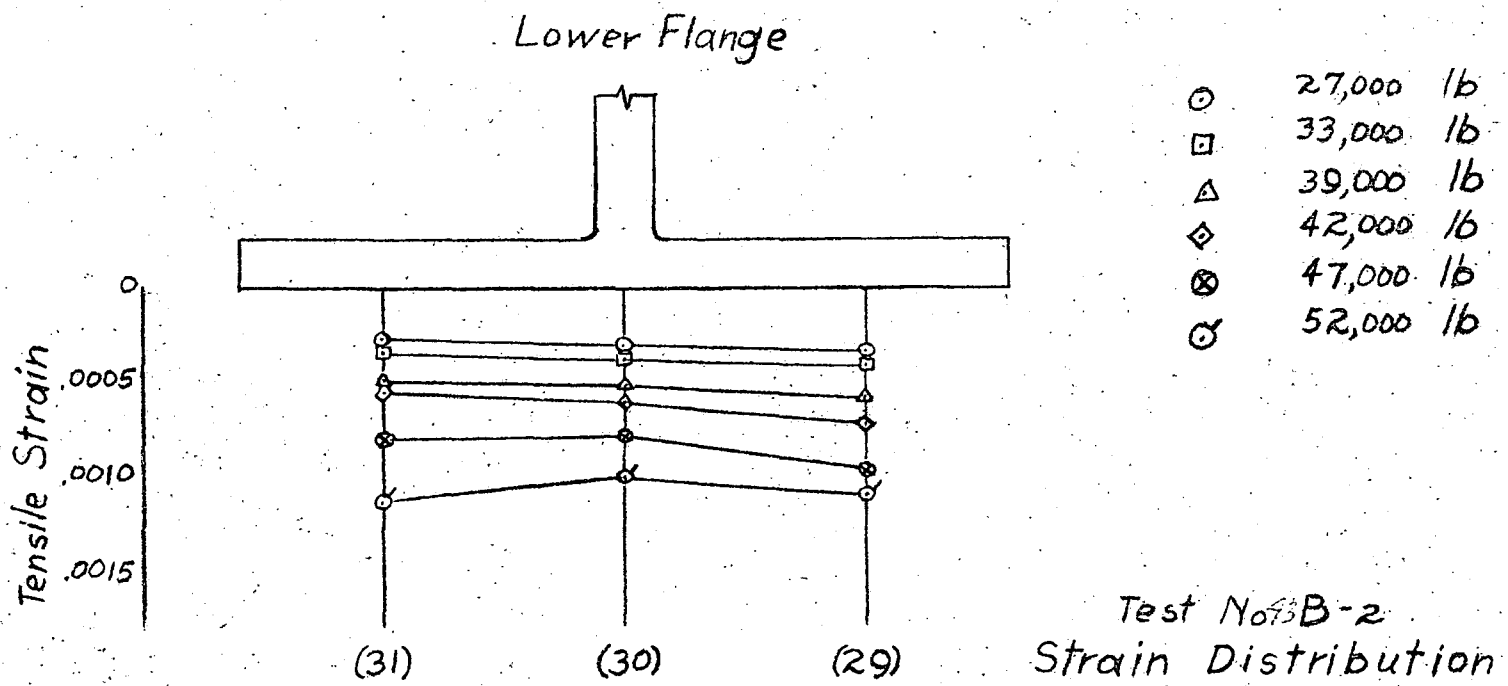
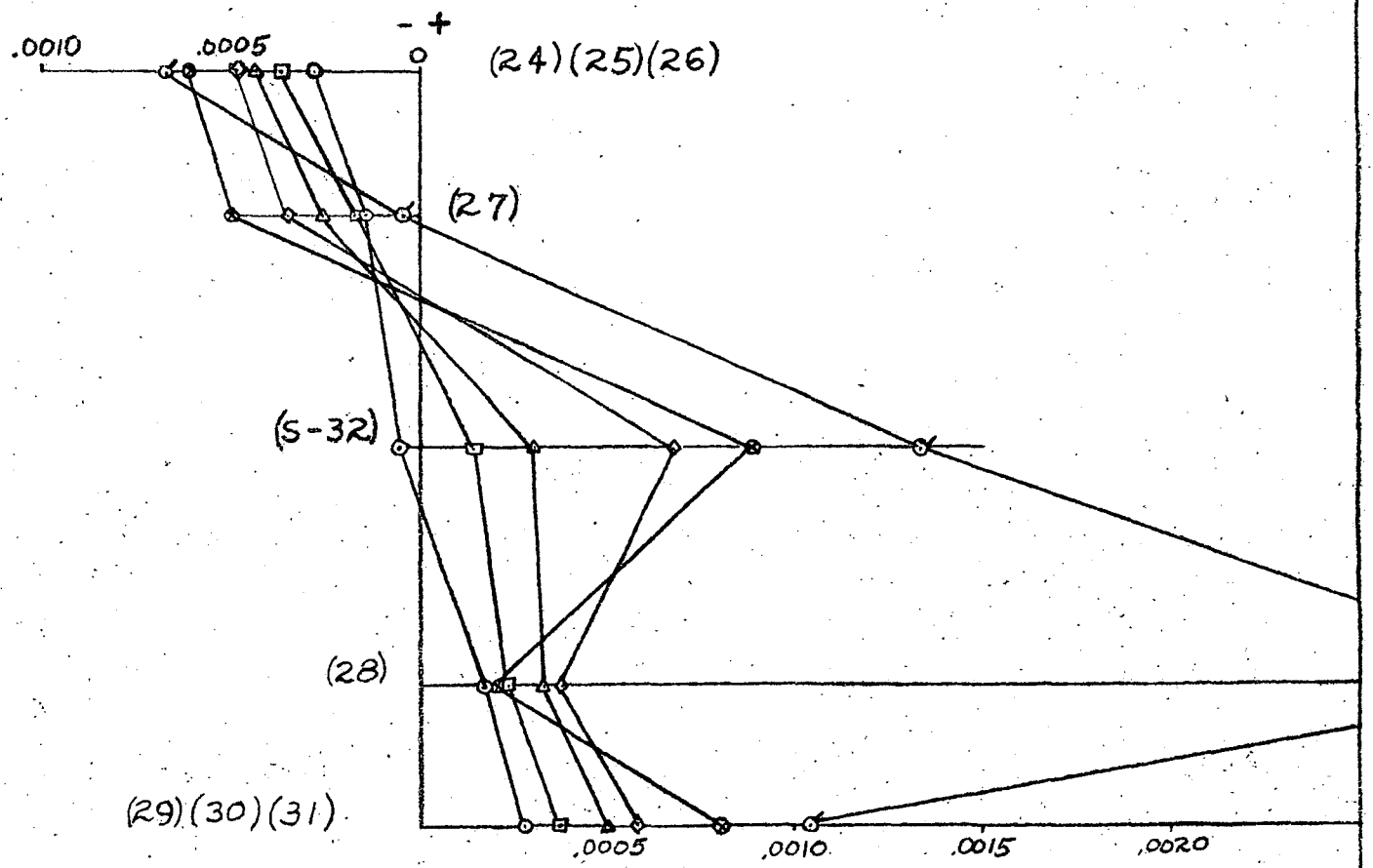
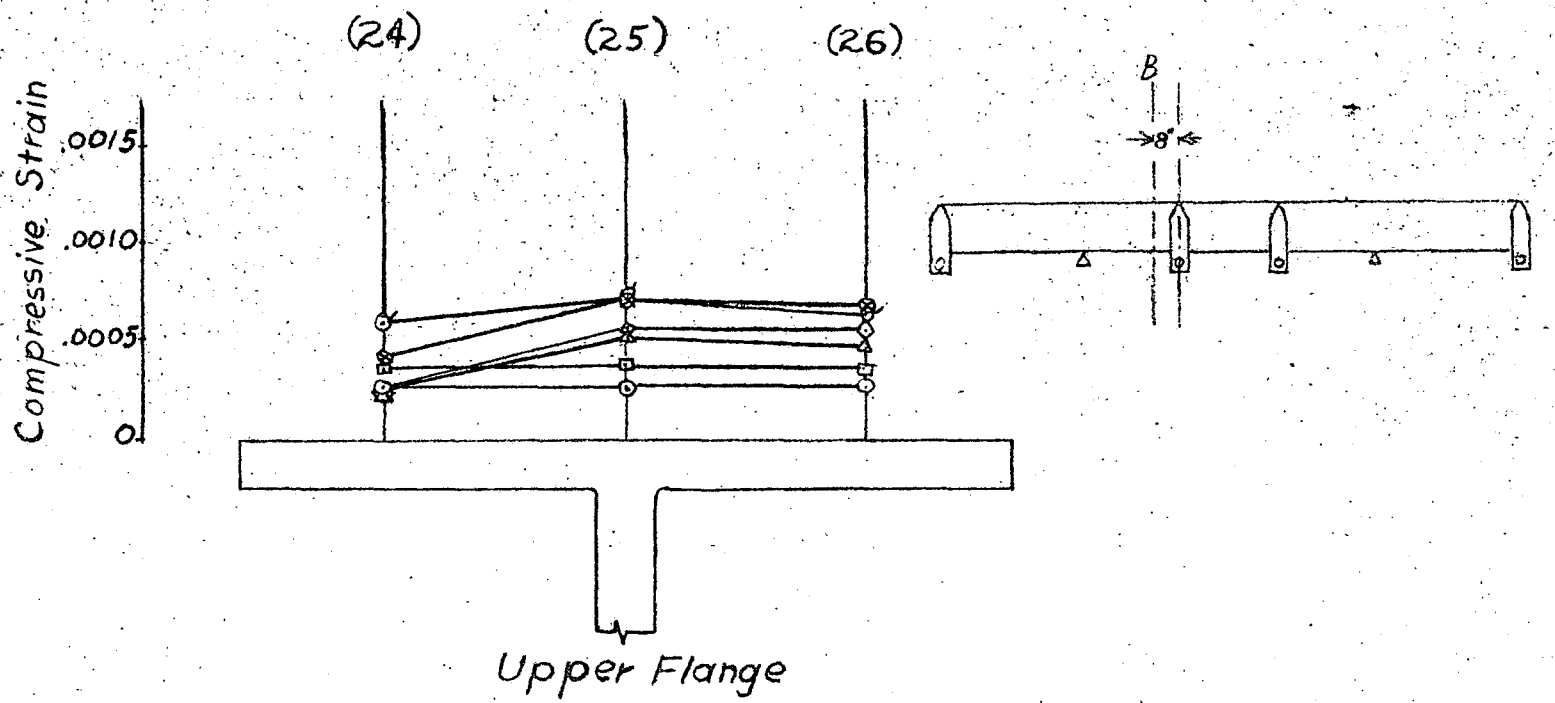


○	27,000 lb
□	33,000 lb
△	39,000 lb
◇	42,000 lb
⊗	47,000 lb

Test No. B-2  
Strain Distribution  
at Section B'  
Fig. 41

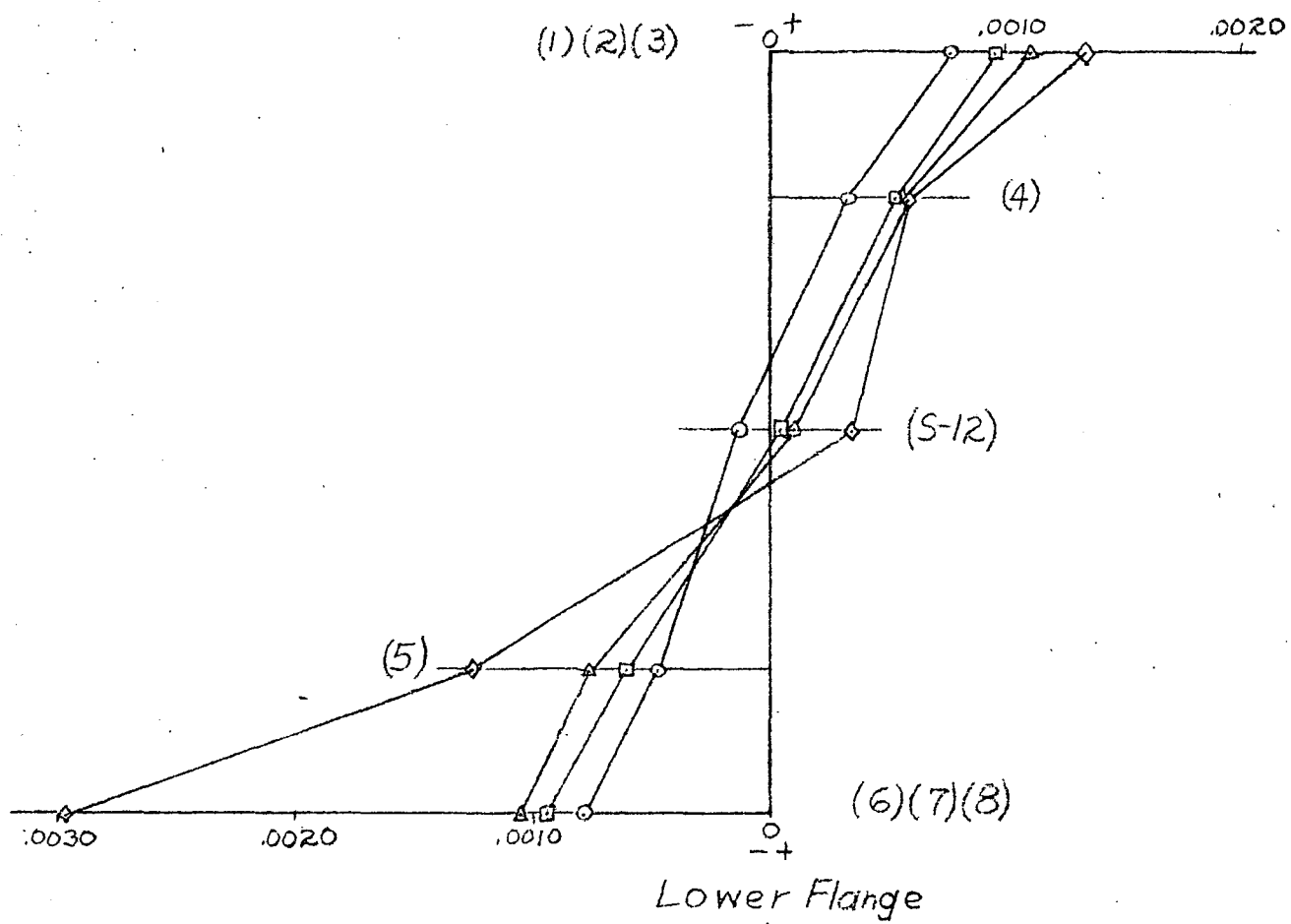
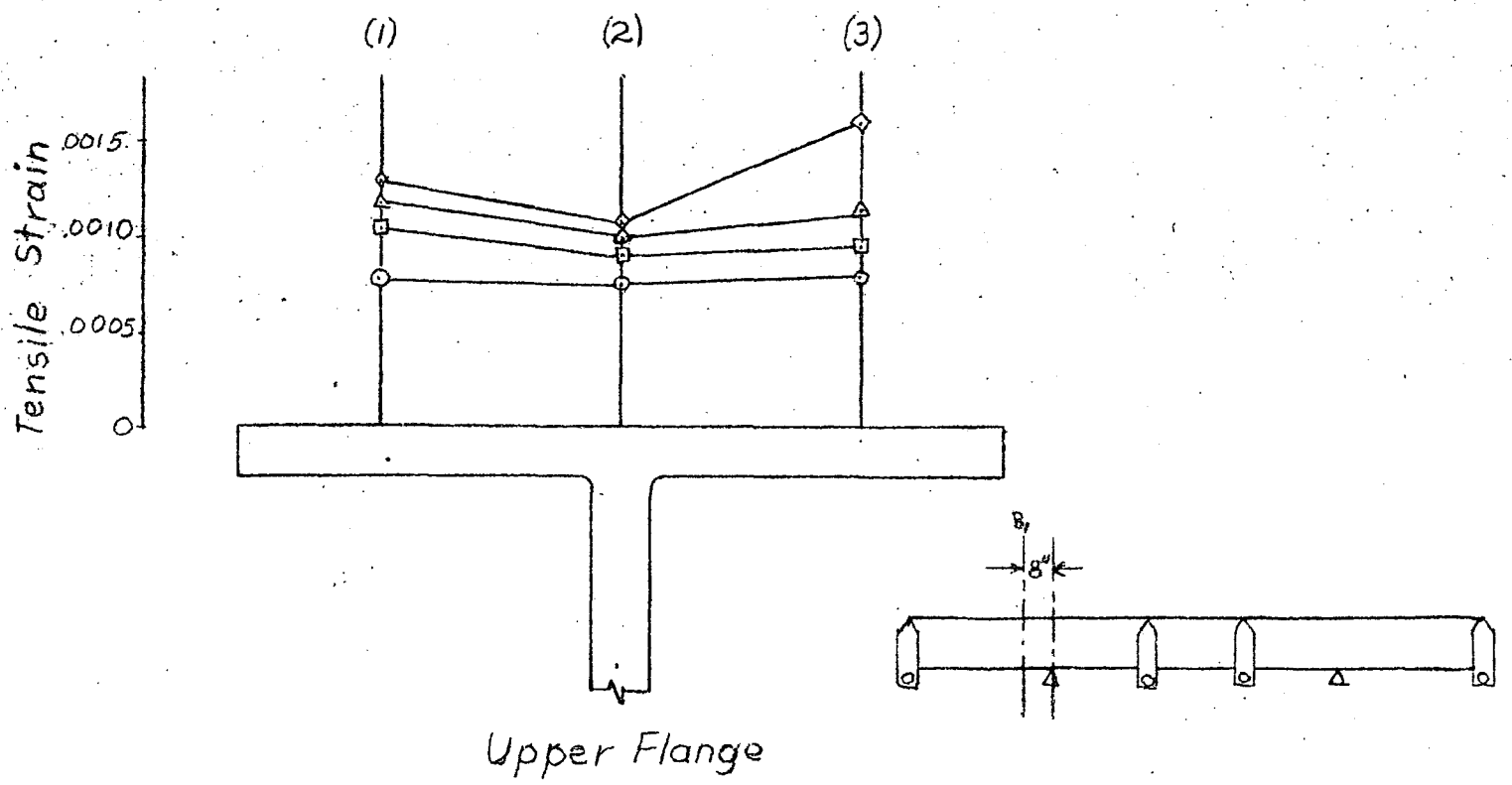




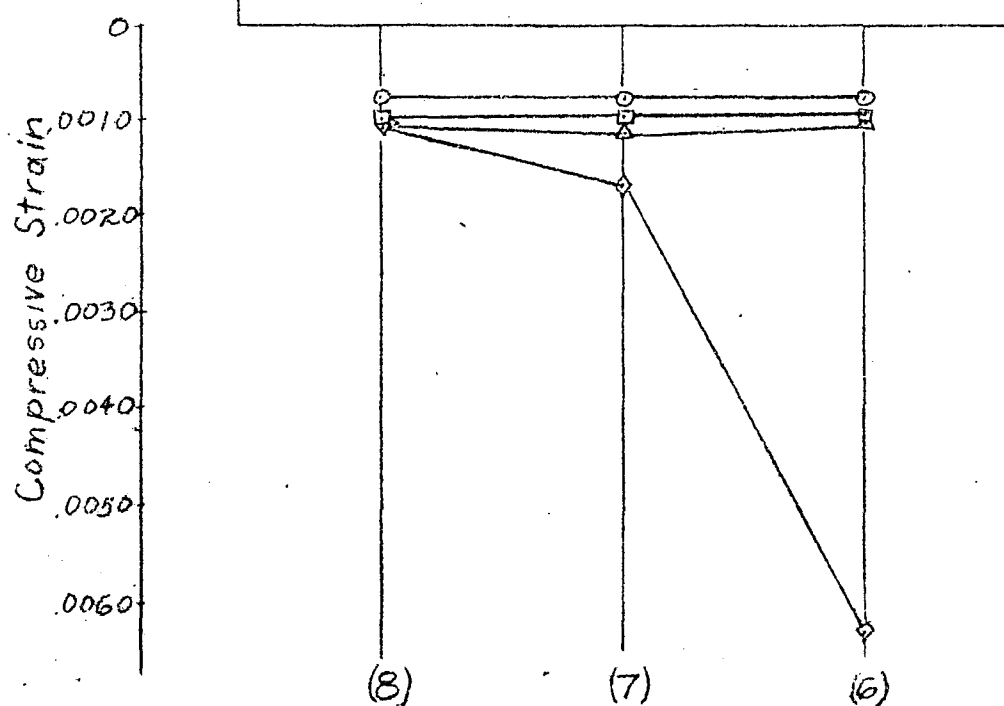


- 27,000 lb
- 33,000 lb
- △ 39,000 lb
- ◇ 42,000 lb
- ⊗ 47,000 lb
- ⊙ 52,000 lb

Test No. B-2  
Strain Distribution  
at Section B  
Fig. 43

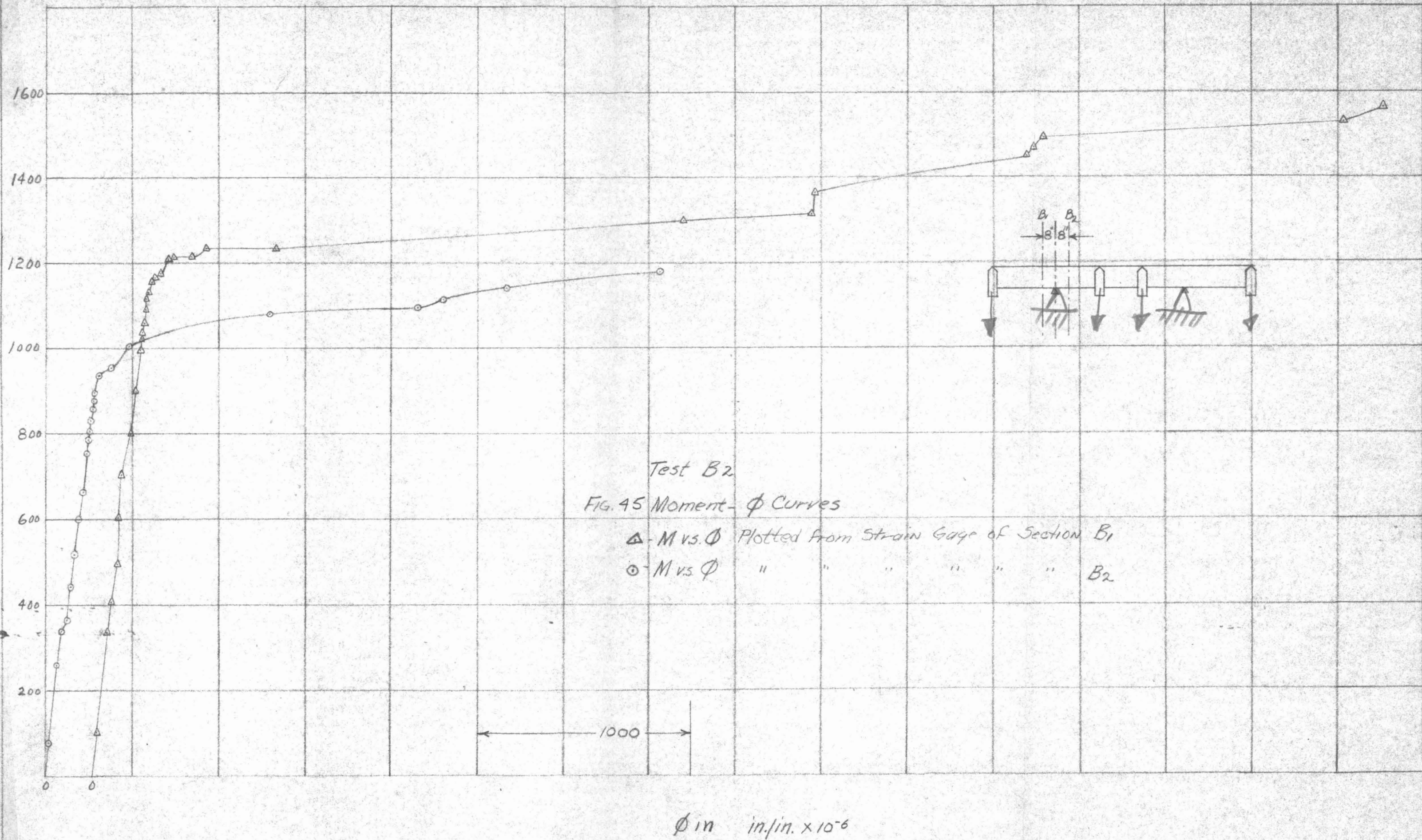


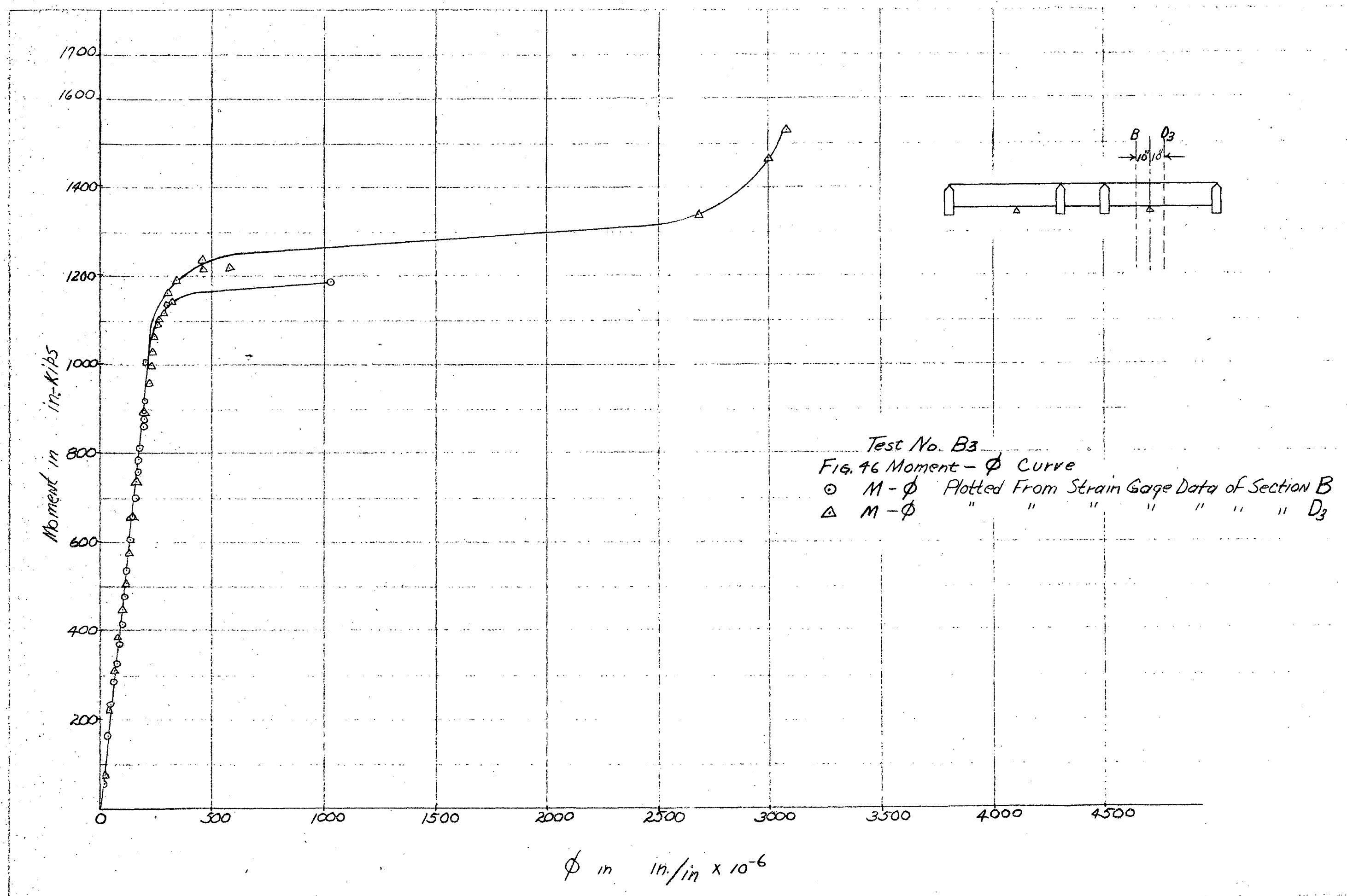
○	27,000 lb
□	33,000 lb
△	39,000 lb
◇	42,000 lb

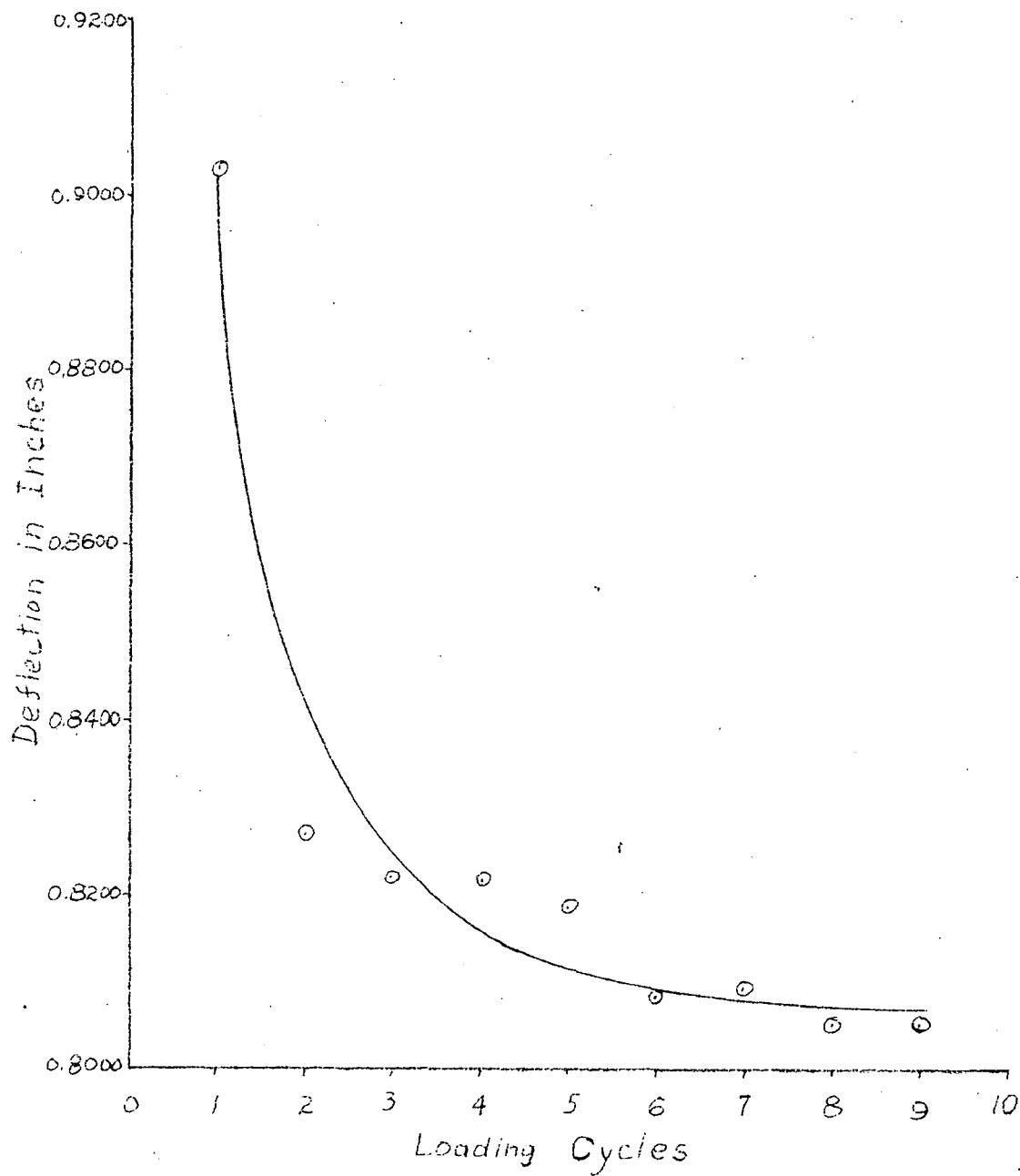


Test No. B-2  
Strain Distribution  
at Section B,  
Fig. 44

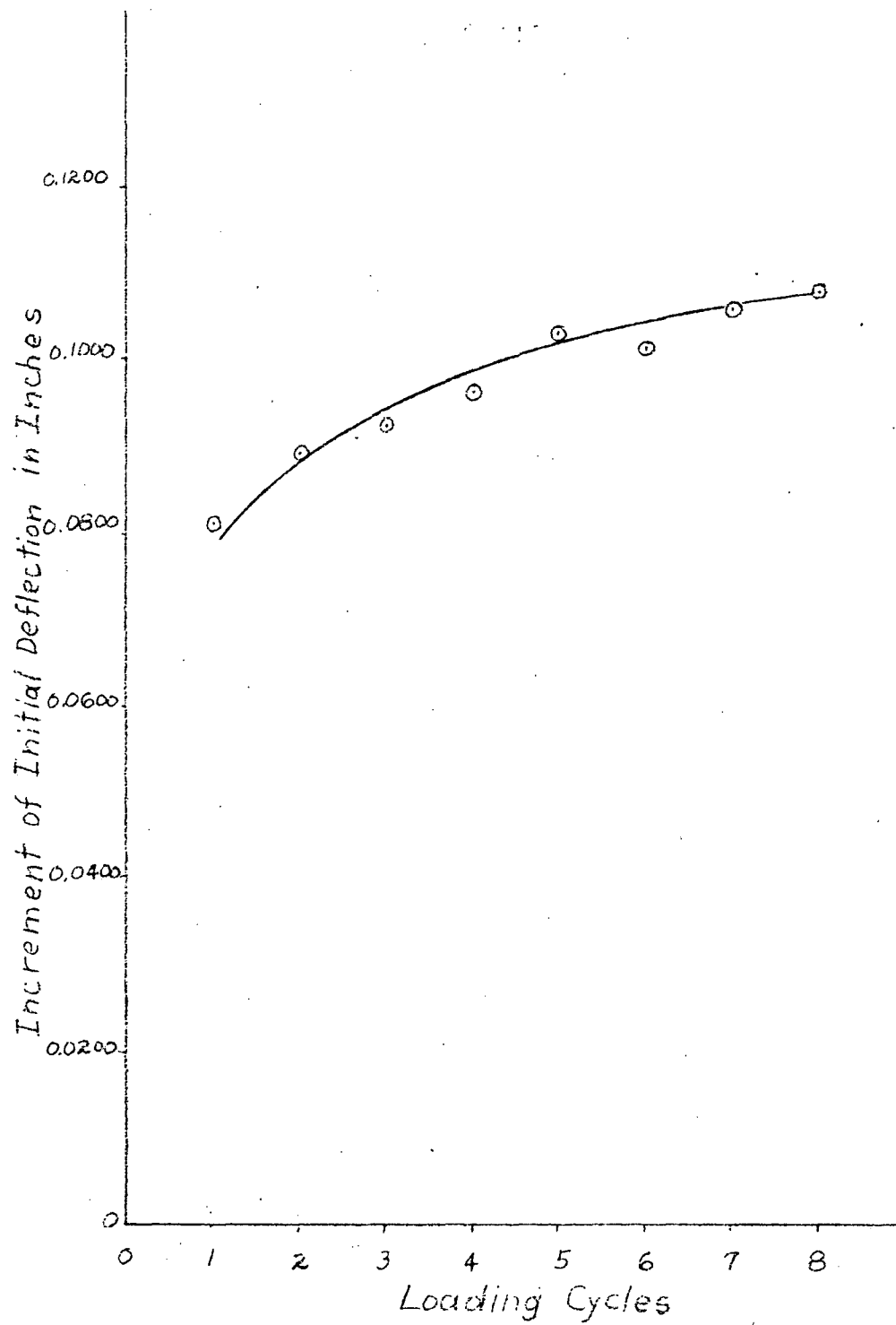








Test No. B<sub>2</sub>  
Fig 47 The Increment of Deflection  
from  $W=3$  Kips to  $W=23$  Kips  
under Repeated Load



Test No. B3  
Fig. 48 Increment of  
Initial Deflection  
under Repeated Load

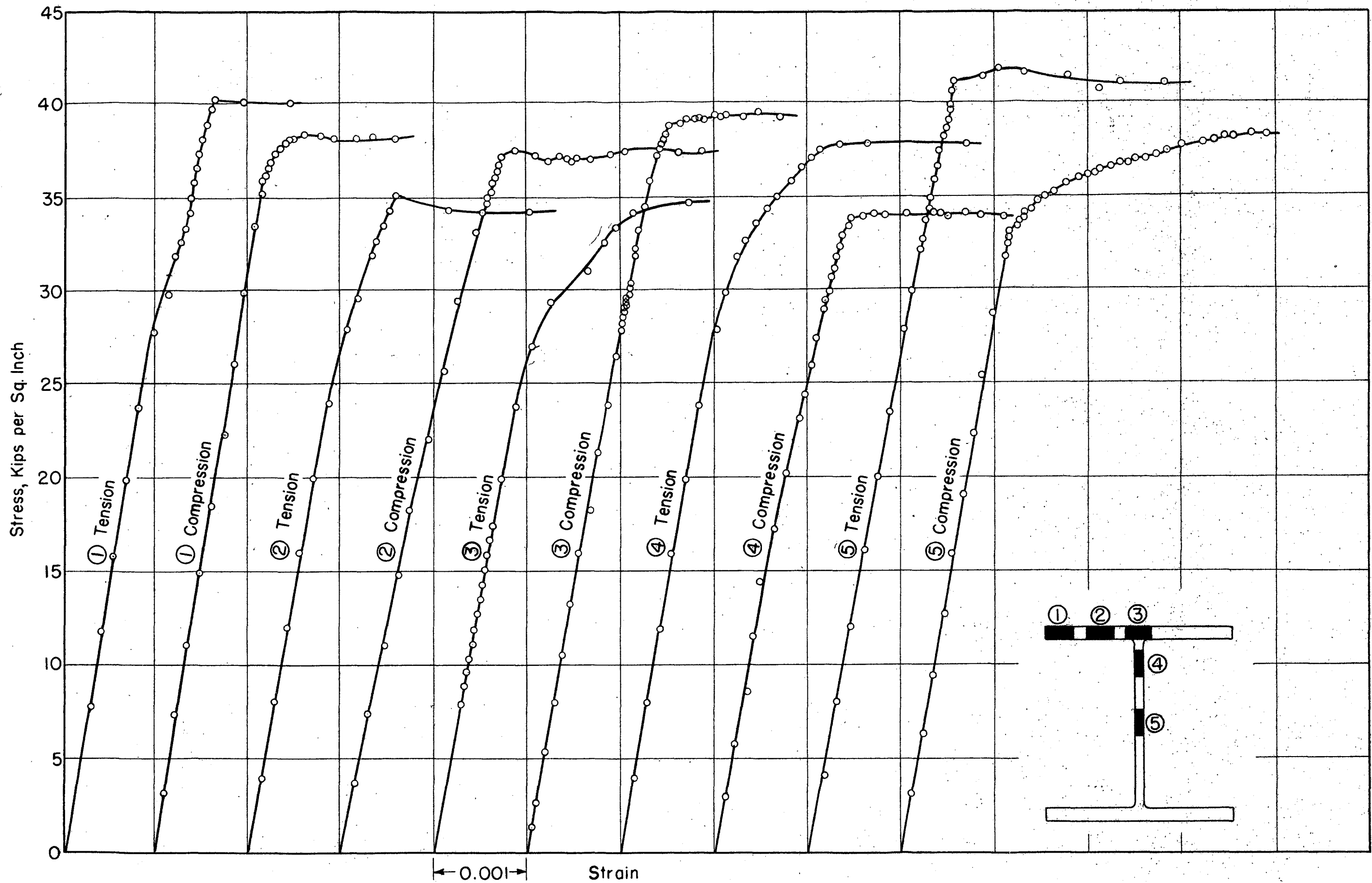


FIG. 49 TENSION AND COMPRESSION STRESS-STRAIN CURVES FOR AN 8W40 BEAM



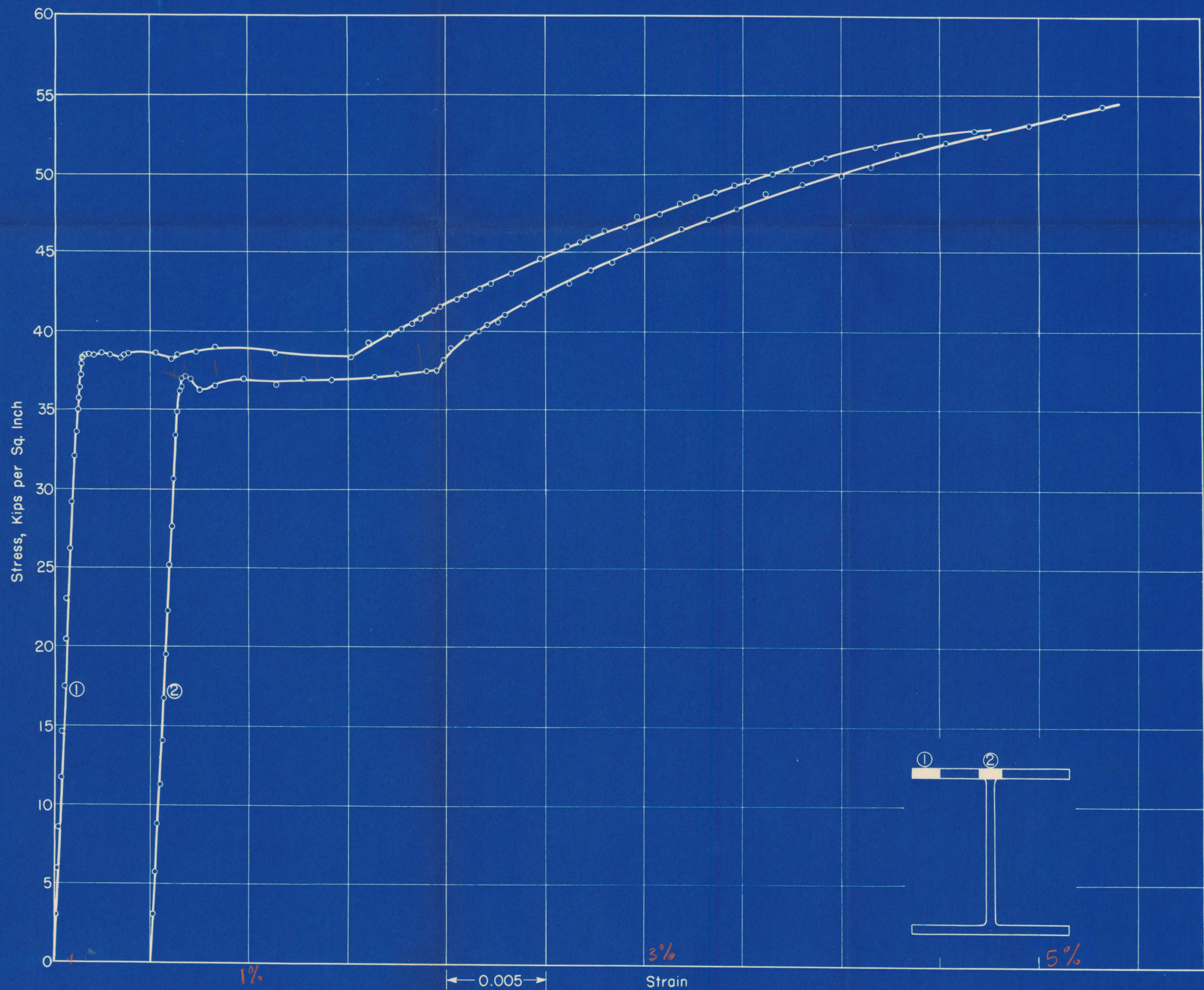


FIG. 50 TENSION STRESS-STRAIN CURVES FOR AN 8WF40 BEAM  
(Including strain-hardening range)